The cIAP ubiquitin ligases sustain type 3 γδ T and innate lymphoid cells during aging to allow normal cutaneous and mucosal responses

John Rizk[1], Urs M. Mörbe[1], Rasmus Agerholm[1], Isabel Ulmert[1], Elisa Catafal Tardos[1], Darshana Kadekar[1], Maria V. Baglioni[1], Monica Torrellas Viñals[1] and Vasileios Bekiaris*[1]

[1]Department of Health Technology, Technical University of Denmark, Kemitorvet, Bldg 202, 2800 Kgs Lyngby, Denmark.

*Corresponding author: Vasileios Bekiaris vasbek@dtu.dk

Abstract

Environmental and molecular cues early in life are often associated with the permanent shaping of our immune system during adulthood. Although increasing, our knowledge of the signaling pathways that operate in early life and their temporal mode of action is limited. Herein, we demonstrate that the cellular inhibitor of apoptosis proteins 1 and 2 (cIAP1/2), which are E3 ubiquitin ligases and master regulators of the nuclear factor-kappa B (NF-κB) pathway, function during late neonatal and prepubescent life to sustain interleukin(IL)-17-producing gamma delta T cells (γδT17) and group 3 innate lymphoid cells (ILC3). We show that cell-intrinsic deficiency in cIAP1/2 at 3-4 weeks of life leads to downregulation of the transcription factors cMAF and RORγt, and failure to enter cytokine-induced cell cycle. This is followed by progressive loss of γδT17 cells and ILC3 while mice are aging. Mice deficient in cIAP1/2 have severely reduced γδT17 cells and ILC3, present with suboptimal γδT17 responses in the skin, lack small intestinal isolated lymphoid follicles and cannot control intestinal bacterial infection. Mechanistically, these effects appear to be dependent on overt activation of the non-canonical NF-κB pathway.

Our data identify the cIAP E3 ubiquitin ligases as critical early life molecular switches for establishing effective type-3 immunity during aging.

Introduction

The neonatal period is the time when our immune system is imprinted with life-long functional characteristics that maintain immunity to infection and prevent autoimmune pathology. Microbial colonization, and developmentally regulated transcriptional programs cooperate to shape innate and adaptive lymphocytes into distinct specialized lineages that co-exist in equilibrium and respond ad hoc (Eberl, 2016). Failure to convey these environmental and molecular cues during neonatal life, often results in irreversible dysfunction later on. Hence, early dysbiosis impairs type-3 immunity and potentiates susceptibility to type-2 driven allergy (Cahenzli *et al*, 2013) . Similarly, blockade of key signaling pathways during neonatal life can permanently change cellular niches (Kadekar *et al*, 2020). Therefore, elucidating the molecular signatures that operate early in life is of great importance for understanding how immunity develops.

Mouse γδ T cells present a well-established example of an immune population that is heavily dependent on an unperturbed neonatal period. In this regard, intestinal intraepithelial (IE) γδ T cells develop during neonatal and prepubescent life through butyrophylin-driven interactions with the epithelia (Di Marco Barros *et al*, 2016) . This provides a necessary defense mechanism against infection within the IEL compartment (Hoytema van Konijnenburg *et al*, 2017). Lamina propria (LP) interleukin(IL)-17-producing γδ T cells establish mixed type-3 and type-1 transcriptional programs within the first week of life through the transcription factor STAT5 (Kadekar *et al*, 2020) . Thus,

early life establishment of the γδT17 compartment is critical to protect from neonatal and adult infections (Chen *et al*, 2020; Sheridan *et al*, 2013). In a similar manner, impaired microbial colonization of the ocular or oral mucosa results in drastically altered IL-17-producing γδ T (γδT17) cell numbers in the conjunctiva (St. Leger *et al*, 2017) and cervical lymph nodes (LN) (Fleming *et al*, 2017). Again, paucity in such γδT17 cell populations is associated with impaired anti-microbial responses in eye and oral cavity (Conti *et al*, 2014; St. Leger *et al*, 2017), and resistance to pathogenic inflammation (Cai *et al*, 2011; Sandrock *et al*, 2018; McGinley *et al*, 2020).

The innate lymphoid cell (ILC) compartment is also dependent on early life events, while their function during the neonatal period is critical for the establishment of the intestinal immune system (Spits *et al*, 2013). In this regard, although dysbiosis does not affect ILC development, it results in altered transcriptional and epigenetic profiles of all ILC subsets (Gury-BenAri *et al*, 2016). Similar to LP γδT17 cells, group 3 ILC (ILC3) acquire expression of the transcription factor Tbet and the type-1 cytokine interferon-γ (IFN-γ) during neonatal life, which allows them to clear intracellular bacterial infections (Klose *et al*, 2013) . Moreover, group 2 ILC (ILC2) undergo an IL-33-dependent maturation step in the neonatal lung, allowing their cytokine responsiveness in adult mice (Steer *et al*, 2020). Importantly, ILC3 induce the maturation of intestinal cryptopathces into isolated lymphoid follicles (ILFs) during the first 3-4 weeks of life (Kiss *et al*, 2011; Kruglov *et al*, 2013). Evidently, perturbations of γδT17 and ILC3 development during the early stages of life will have a substantial impact on the quality of immunity while aging. The molecular pathways that control the transition of these cells from neonatal life to adolescence and adulthood are poorly understood.

72 The E3 ubiquitin ligases cellular inhibitor of apoptosis protein (cIAP)1 and 2
73 (cIAP1/2) catalyze both degradative lysine(K)-48 and stabilizing K-63 ubiquitination and
74 act as the main molecular switches for the activation of the canonical and non-canonical
75 nuclear factor-kappa B (NF-κB) pathway (Silke & Meier, 2013) . The presence of
76 cIAP1/2 downstream of TNF receptor 1 (TNFR1) determines whether a cell will initiate
77 the canonical NF-κB pathway or die by apoptosis or necroptosis in response to TNF
78 (Annibaldi & Meier, 2018). They achieve this by ubiquitinating receptor interacting
79 kinase-1 (RIPK1) (Silke & Meier, 2013) . However, cIAP1/2 are mostly recognized as
80 negative regulators of the non-canonical NF-κB pathway. Hence, in all cell types
81 cIAP1/2 associate in a heterocomplex with TNF receptor associated factor (TRAF)2,
82 TRAF3 and NF-κB-inducing kinase (NIK), whereby they induce K-48 ubiquitination of
83 NIK, resulting in its continuous proteasomal degradation (Zarnegar *et al*, 2008;
84 Varfolomeev *et al*, 2007; Vince *et al*, 2007). Breakdown of the TRAF2-TRAF3-cIAP1/2-
85 NIK complex either following ligation of TNF superfamily receptors that recruit TRAF2-
86 TRAF3 in their intracellular domain (e.g. TNFR2, LTβR, CD40) or by cIAP1/2 depletion,
87 liberates NIK, which initiates the cascade necessary for nuclear translocation of the
88 non-canonical NF-κB transcription factors RelB and p52 (Vallabhapurapu *et al*, 2008;
89 Matsuzawa *et al*, 2008)
90 In the present study we demonstrate a necessary role for cIAP1/2 in sustaining
91 γδT17 cells and ILC3 at the late neonatal and prepubescent stages of life, and thus
92 impacting the magnitude of inflammatory and anti-bacterial immune responses.
93 Deficiency in cIAP1/2 begun to have an impact only during late neonatal life by reducing
94 expression of the lineage defining transcription factors cMAF and RORγt, which was
95 followed by an apparent block in cytokine-induced proliferation. When animals entered

96 prepubescence and early adolescence, cIAP1/2 deficiency resulted in progressive loss
97 γδT17 cells. This was independent of TNFR1 induced canonical NF-κB or cell death. In
98 contrast, cIAP1/2-deficient prepubescent γδT17 cells displayed enhanced nuclear
99 translocation of RelB, which demonstrates evidence of overt activation of the non-
100 canonical NF-κB pathway. Intestinal ILC3 also relied on intact cIAP1/2 during the same
101 time period, with their numbers being drastically reduced in adulthood. Paucity in ILC3
102 coincided with ILF involution. Mice with targeted deletion of cIAP1/2 in γδT17 cells and
103 ILC3 responded sub-optimally to cutaneous inflammatory challenge and failed to control
104 intestinal bacterial infection.
105
106 **Results**
107 **Paucity of γδT17 cells in the absence of the E3 ubiquitin ligases cIAP1 and cIAP2**
108 Using acute, SMAC mimetic (SM) driven antagonization and in vitro techniques, we
109 showed before that cIAP1/2 are important for T_H17 differentiation through modulation of
110 the non-canonical NF-κB pathway (Rizk *et al*, 2019). In order to understand the in vivo
111 importance of cIAP1 and cIAP2 in RORγt-expressing immune cells, we crossed *Rorc*-
112 Cre (RORγt^{CRE}) mice (Eberl & Litman, 2004) with mice that were floxed for *Birc2*
113 (cIAP1$^{F/F}$) and knocked out for *Birc3* (cIAP2$^{-/-}$) (Gardam *et al*, 2011). This generated
114 mice with RORγt-driven deletion of cIAP1 (referred to thereafter as ΔIAP1) and
115 generalized deletion of cIAP2 (referred to thereafter as ΔIAP2), as well as the
116 corresponding Cre-negative littermate controls (wild-type; WT) (Fig 1A). ΔIAP1 and
117 ΔIAP1/2 mice were viable, produced offspring at expected rates, and did not develop
118 any observable spontaneous disease phenotypes. They contained a full set of lymph
119 nodes (inguinal, brachial, axillary and mesenteric) and Peyer's patches indicating

120 unperturbed lymphoid tissue development, while total numbers of $CD4^+$ T and B cells
121 were normal but γδ T were slightly elevated (Fig S1A).
122 We next analyzed some of the major IL-17-producing populations in lymph node
123 (LN) and small intestinal and colonic lamina propria (siLP; cLP). Compared to littermate
124 controls, ΔIAP1/2 mice produced slightly elevated levels of IL-17A within the
125 $CD4^+TCR\beta^+$ compartment in the LN (pool of inguinal, brachial, axillary) but not the gut
126 (Fig S1B), suggesting that in these animals, steady-state production of IL-17A by $CD4^+$
127 T cells is not defective. Staining for IL-22 following overnight stimulation with IL-23
128 yielded the same answer (Fig S1C). However, there was a marked reduction in γδ-
129 associated IL-17A and IL-22 production in LN (Fig 1B) and IL-17A in the gut (Fig 1C).
130 This was accompanied by a dramatic loss in LN $TCR\gamma\delta^+CD27^-CD44^{hi}CCR6^+$, which are
131 the IL-17-producing γδ T cells (Ribot *et al*, 2009; Haas *et al*, 2009) (Fig 1D and Fig
132 S1D), and gut $Tbet^+ROR\gamma t^+$ (Kadekar *et al*, 2020) (Fig 1E) γδT17 cell numbers.
133 Although cIAP1 and cIAP2 individually did not contribute to this phenotype in the LN,
134 ΔIAP2 mice had significantly reduced $Tbet^+ROR\gamma t^+$ γδ T cell numbers in the gut (Fig
135 1E). We additionally found significantly reduced γδT17 cells in the lungs of ΔIAP2 mice
136 (Fig S1E). Similar to γδT17 cells, there were significantly reduced non-CD4 IL-17-
137 producing lymphocytes in the LNs of ΔIAP1/2 mice (Fig S1F).
138 In the skin, $CD3^{lo}V\gamma5^-TCR\gamma\delta^+CCR6^+$ cells, which represent the γδT17 population
139 (Haas *et al*, 2009, 2012), were also reduced significantly in the absence of cIAP1 and
140 cIAP2 (Fig 2A). When we analyzed the two major γδT17 subpopulations ($V\gamma4^+$ versus
141 $V\gamma4^-$; Vγ nomenclature by Heilig and Tonegawa; (Heilig & Tonegawa, 1986)), we found
142 that in the skin cIAP1 but not cIAP2 was required for $V\gamma4^-$ cells, whereas the Vγ4-
143 expressing population was only affected by the absence of both cIAP1 and cIAP2 (Fig

144 2B). In the LN, we did not observe differential regulation of either Vγ4$^+$ or Vγ4$^-$ cells (Fig
145 S2A). Collectively, this data suggests that cIAP1/2 are important for the development
146 and/or homeostatic maintenance of γδT17 cells. Our findings additionally pinpoint a
147 differential and non-redundant role of cIAP1 and cIAP2 in these cells that is organ and
148 subset specific. In this regard, whereas skin γδT17 cells depended more on cIAP1, gut
149 γδT17 cells depended more on cIAP2.
150

151 **Cell-intrinsic requirement for cIAP1 and cIAP2 in γδT17 cells**

152 Next, we investigated whether the defect we observed in ΔIAP1/2 mice was cell-
153 intrinsic. To this end we set up mixed bone marrow (BM) chimeras where WT
154 CD45.1$^+$CD45.2$^+$ hosts were sub-lethally irradiated and reconstituted with a mixture of
155 1:1 CD45.1$^+$ WT and CD45.2$^+$ ΔIAP1/2 BM cells (Fig 3A). We found that, under these
156 conditions, WT LN γδT17 cells outcompeted their ΔIAP1/2 counterparts (Fig 3B),
157 indicating the phenotype we observed in intact mice was cell intrinsic. Interestingly,
158 CD27$^+$ γδ T cells derived from ΔIAP1/2 BM were slightly less competitive than WT (Fig
159 3B). In contrast, both CD3$^-$ populations and B cells from ΔIAP1/2 BM were more
160 competitive than their WT counterparts (Fig 3C). This indicated that the reduced
161 competitiveness of γδT17 and CD27$^+$ γδ T cells was not due to defective ΔIAP1/2 BM
162 reconstitution. We could not reconstitute gut RORγt$^+$Tbet$^+$ γδT17 cells irrespective of
163 the BM source (Fig 3D), suggesting that this population requires either thymus-
164 originated γδ T cells or a neonatal microenvironment to develop fully. In contrast, lack of
165 cIAP1 and cIAP2 did not impinge on the reconstitution of gut Tbet$^+$RORγt$^-$ γδ T cells
166 (Fig 3E). Likewise, we could only recover WT LN γδT17 cells when we reconstituted
167 ΔIAP1/2 hosts with WT or a 1:1 mix of WT and ΔIAP1/2 BM (Fig S3A-B), while CD27$^+$

168 γδ T cells from WT or ΔIAP1/2 BM cells were equally competitive (Fig S3B). As before,
169 we could not reconstitute RORγt^{+}Tbet^{+} γδT17 cells in the gut (Fig S3C).
170 As γδT17 cells develop perinatally in the thymus and undergo a rapid neonatal re-
171 programming within the tissues they localize at, we reasoned that if generated from BM
172 stem cells, they might have different developmental or homeostatic requirements for
173 cIAP1 and cIAP2. To address this issue, we purified γδ T cells from the thymi of 1-day
174 old WT or ΔIAP1/2 mice and transferred them to RAG1$^{-/-}$ recipients (Fig 3F). We found
175 that 12 weeks post transfer, the γδT17 cell compartment was reconstituted in the LN,
176 however, we recovered significantly more WT than ΔIAP1/2 cells (Fig 3G). As with the
177 BM chimeras, we could not reconstitute intestinal RORγt^{+}Tbet^{+} γδT17 cells, suggesting
178 that this population requires a neonatal microenvironment (Fig S3D). Reconstitution of
179 CD27^{+} γδ T cells was independent of cIAP1 and cIAP2 (Fig 3G). Taken together our
180 data show that γδT17 cells require cIAP1 and cIAP2 intrinsically.
181
182 **The impact of cIAP1 and cIAP2 on γδT17 cells is independent of TNF induced**
183 **canonical NF-κB and cell death**
184 In addition to preventing spontaneous activation of the non-canonical NF-κB pathway,
185 cIAP1/2 are necessary to convey the canonical NF-κB downstream of TNFR1 whereas
186 in their absence, TNF-TNFR1 interactions can lead to RIPK1-mediated cell death via
187 apoptosis or necroptosis (Annibaldi & Meier, 2018). Mice deficient in TNFR1 had an
188 intact γδT17 cell population (Fig S4A), suggesting that the canonical NF-κB pathway
189 downstream of TNFR1 is not responsible for the phenotype of ΔIAP1/2 mice. Since TNF
190 is highly upregulated during the weaning reaction (Al Nabhani *et al*, 2019), we next
191 investigated whether TNF induced cell death played a role. To achieve this, we initially

192 analyzed mice that were deficient in cIAP2 and expressed a ubiquitin-associated (UBA)
193 domain mutant form of cIAP1 unable to K48 ubiquitylate and suppress RIPK1 (Annibaldi
194 *et al*, 2018). Thus, these mice are more sensitive to TNF induced cell death (Annibaldi
195 *et al*, 2018). In UBA-mutant mice, γδT17 cells were not affected (Fig S4B), suggesting
196 that these cells are not susceptible to death by homeostatic levels of TNF. In order to
197 test this directly in ΔIAP1/2 mice, we began injecting 1-week old neonates with
198 neutralizing anti-TNF antibody and until animals were 12-week old (Fig S4C). We could
199 not rescue the γδT17 population in either gut or LNs (Fig S4D-E), indicating that TNF
200 induced death is unlikely to play a major role in regulating these cells in the absence of
201 cIAP1/2. Therefore, TNF-TNFR1 interactions are not responsible for the ΔIAP1/2
202 phenotype, suggesting that overt activation of the non-canonical NF-κB pathway could
203 play a key role.
204
205 **cIAP1 and cIAP2 are required for γδT17 cell cycle progression and expression of**
206 **cMAF and RORγt during aging**
207 In order to assess the impact of cIAP1/2 on embryonic γδT17 cell development, we
208 enumerated thymic cell numbers in newborn ΔIAP1/2 mice and found them similar to
209 littermate controls (Fig 4A), despite efficient deletion of *Birc2* (cIAP1) (Fig S5A).
210 Production of IL-17A/F were unchanged at this stage (Fig S5B). This suggested that the
211 major impact of cIAP1/2 occurs post-embryonically. We therefore tracked LN γδT17
212 cells, defined phenotypically as $CD27^{-}CD44^{hi}$, during neonatal, post-neonatal (average
213 weaning time at 3 weeks) and adult life (mating age of 8 weeks). We did not find any
214 differences in cell numbers until week 5 of age (Fig 4B). This suggested that cIAP1 and
215 cIAP2 are only required to sustain γδT17 numbers following weaning. After week 5,

216 ΔIAP1/2 γδT17 cells failed to expand and began to decline progressively during aging
217 (Fig 4B). In order to confirm that the cells are missing from adult life and have not
218 converted to a non-γδT17 population, we crossed ΔIAP1/2 with the ROSA26-LSL-RFP
219 strain, so that RFP permanently marks all current and "ex" RORγt-expressing cells. We
220 found no evidence of γδT17 conversion to other populations (Fig 4C). This data
221 suggested that cIAP1/2 regulate a checkpoint in early adult life that manifests during
222 aging.

223 We next investigated what this checkpoint was. The inability of the cells to increase
224 in numbers during aging, raised the hypothesis that cIAP1/2 may be regulating
225 responsiveness to cytokines that induce proliferation. We thus isolated 4-week old LN
226 cells and treated them in vitro with IL-7 or a combination of IL-1β+IL-23. We found that
227 ΔIAP1/2 γδT17 cells were slower in entering cell cycle with most cells stuck in G0 (Fig
228 4D-E). This defect in proliferation was also observed following stimulation with either IL-
229 2 or TCR cross-linking (Fig S5C). Therefore, cIAP1/2 are important for γδT17 cell cycle
230 progression.

231 We have shown before that ablation of cIAP1/2 in T cells downregulates cMAF, a
232 lineage determining transcription factor for γδT17 cells (Zuberbuehler *et al*, 2019), in a
233 NIK- and RelB-dependent mechanism (Rizk *et al*, 2019). We thus hypothesized that
234 lack of cIAP1/2 may influence expression of cMAF. In newborn thymus expression of
235 cMAF as well as RORγt was unchanged (Fig S6A). At week 1 after birth we observed a
236 slight reduction in the expression of RORγt and cMAF (Fig S6B). However, at week 3 of
237 age, expression of RORγt and cMAF was significantly reduced (Fig 5A). Furthermore,
238 we observed a modest but significant reduction in IL-17A production by 3-week old
239 ΔIAP1/2 γδT17 cells (Fig 5B). In the intestine, RORγt^{+} γδ T cells express high levels of

240 CD127 (IL-7Rα) and intermediate levels of CD45 (Fig 5C). Due to lack of other reliable
241 surface markers to identify these cells in the gut, we gated TCRγδ^{+}CD45^{int}CD127^{+} cells
242 and quantified numbers as well as expression of RORγt and cMAF. Similar to the LNs,
243 numbers in the siLP did not change in 4-week old ΔIAP1/2 mice (Fig 5D), however there
244 was a significant reduction in the levels of RORγt and cMAF (Fig 5E).

245 Furthermore, we investigated the expression of RelB in newborn thymic γδ T cells
246 and found a significant upregulation of *Relb* mRNA in ΔIAP1/2 γδT17 but not in CD27^{+}
247 γδ T cells (Fig S6C). We additionally examined the extent of RelB nuclear translocation
248 in γδT17 cells from 4-week old WT, ΔIAP2 and ΔIAP1/2 mice. We found that the levels
249 of nuclear RelB in ΔIAP1/2 γδT17 cells were significantly higher by comparison to WT
250 cells (Fig 5F), arguing for a role of the non-canonical NF-κB pathway in downregulation
251 of RORγt and cMAF. Therefore, cIAP1/2 are required during late neonatal life in order to
252 maintain expression of the transcription factors RORγt and cMAF and to sustain normal
253 γδT17 numbers.

254

255 **Inflammation partially restores γδT17 responses in the absence of cIAP1 and**
256 **cIAP2**

257 Next, we investigated whether cytokines that activate γδT17 cells could regulate
258 expression of RORγt and cMAF from 4-week old mice. Culture with IL-7 did not
259 influence expression of either transcription factors (Fig 6A-C), however, a combination
260 of IL-1β and IL-23 resulted in partial restoration of RORγt but not cMAF in ΔIAP1/2
261 γδT17 cells (Fig 6A-C). Interestingly, IL-1β+IL-23 resulted in downregulation of cMAF in
262 WT cells (Fig 6A-B). We additionally observed that the ΔIAP1/2 γδT17 cells that
263 acquired RORγt, were the cells that entered G1 in response to IL-1β+IL-23 and to a

264 lesser extent in response to IL-7 (Fig S7). In the imiquimod(IMQ)-driven psoriasiform
265 dermatitis model, IL-23, IL-1β and IL-7 drive γδT17 cell expansion as well as production
266 of IL-17 and IL-22 in the LN and skin (Michel *et al*, 2012; Cai *et al*, 2011, 2014). We thus
267 treated WT, ΔIAP1, ΔIAP2, and ΔIAP1/2 4-week old mice with IMQ for seven days and
268 assessed expression of RORγt and cMAF in γδT17 cells. We found that IMQ treatment
269 partially restored expression of both RORγt and cMAF in ΔIAP1/2 γδT17 cells in the
270 LNs (Fig 6D), suggesting that inflammation can rescue the ΔIAP1/2 phenotype.
271 We then investigated whether rescue of RORγt and cMAF was sufficient for
272 ΔIAP1/2 γδT17 cells to mount an immune response. We observed that despite an
273 increase in Ki67 expression (Fig S8A), ΔIAP1/2 γδT17 numbers did not increase in
274 either the LNs or skin (Fig 6E). Evaluation of cytokine production revealed substantial
275 regional differences between LN and skin in ΔIAP1/2 mice. Thus, whereas in the LN,
276 ΔIAP1/2 γδT17 cells increased (albeit significantly less than their WT, ΔIAP1 and ΔIAP2
277 counterparts) their production of IL-17A following IMQ treatment, this was not the case
278 in the skin (Fig 6F). In contrast, IL-22 production in LNs was significantly reduced while
279 it was relatively normal in the skin (Fig 6G). The $CD4^+$ T cell response to IMQ was not
280 defective and slightly stronger in ΔIAP1/2 mice (Fig S8B). The extent of skin
281 inflammation, as measured by epidermal thickening, was not different between ΔIAP1/2
282 and control mice, reflecting both the partial rescue of the γδT17 as well as the slightly
283 exaggerated $CD4^+$ T cell response (Fig S8C).
284 The data suggest that although at a young age cIAP1/2 regulate proliferation,
285 transcriptional stability and cytokine production, strong inflammatory stimuli can, to a
286 certain extent, overcome this regulatory checkpoint and revive γδT17 cell responses.
287 These results additionally indicate that the extrathymic expression and biological impact

288 thereafter of RORγt and cMAF can be dynamic and under the control of multiple
289 microenvironment cues.
290
291 **cIAP1 and cIAP2 are required for intestinal ILC3 during aging and for sustaining**
292 **ILF integrity**
293 ILC3 share many functional characteristics and transcription factor requirements with
294 γδT17 cells, including constitutive expression of RORγt and cMAF (Zuberbuehler *et al*,
295 2019; Parker *et al*, 2019). We therefore investigated the impact of cIAP1 and cIAP2
296 deficiency in intestinal ILC3 populations. Similar to γδT17 cells, LP Tbet^{+} and Tbet^{-} ILC3
297 numbers were reduced in ΔIAP1/2 mice (Fig 7A-C and Fig S9A). As expected ILC2
298 numbers were not affected (Fig S9B). Next, we tested whether ΔIAP1/2 ILC3 converted
299 to an RORγt^{-} population and hence performed a lineage tracing experiment using the
300 RORγt-RFP reporter mice described above. We found that within the ILC population,
301 there was a 10-fold reduction in RFP^{+} cell numbers, suggesting that in the absence of
302 cIAP1 and cIAP2, there is loss of ILC3 rather than conversion to a non-ILC3 population
303 (Fig S9C). Similar to γδT17 cells, we found that ILC3 numbers did not expand post
304 weaning (Fig 7D). Next, we investigated whether the ILC3 defect in ΔIAP1/2 mice was
305 cell-intrinsic. To this end, using mixed BM chimeras, we found that WT ILC3
306 outcompeted their ΔIAP1/2 counterparts (Fig 7E-F), indicating that the phenotype we
307 observed in intact mice was cell-intrinsic. There was equal reconstitution capacity of
308 GATA3-expressing ILC2 derived from WT or ΔIAP1/2 BM (Fig S9D), demonstrating the
309 specificity of the defect within RORγt-expressing populations. We obtained similar
310 results when we reconstituted ΔIAP1/2 hosts with a 1:1 mix of WT and ΔIAP1/2 BM (Fig

311 7G and Fig S9E). Further, cIAP1 and 2 deficient ILC3 cells were not rescued by
312 treatment with anti-TNF (Fig S9F).
313 ILC3 are necessary for the maturation of cryptopatches to ILFs during the first
314 weeks of life. ΔIAP1/2 mice had severely defective ILFs (Fig 7H). ILFs in these mice
315 were either absent or reduced in size (Fig 7H). Despite the lack of ILFs, production of
316 IgA was not defective (Fig S9G). Collectively, this data shows that cIAP1 and cIAP2 are
317 necessary for intestinal ILC3 to expand during the post-weaning period, and to induce
318 formation of ILFs.
319
320 **cIAP1 and cIAP2 are necessary to protect against *Citrobacter rodentium* infection**
321 It has been demonstrated that ILC3 are important to control infection by the attaching
322 and effacing bacterium *Citrobacter rodentium* (Bauché *et al*, 2020; Guo *et al*, 2015,
323 2014), a widely used model for human enteropathogenic *E. coli* infections (Silberger *et*
324 *al*, 2017) .We therefore reasoned that ΔIAP1/2 mice may be defective in mounting a
325 protective response to *C. rodentium*. We infected ΔIAP1/2 mice and their respective
326 controls with $2x10^9$ CFU of *C. rodentium* through oral gavage and followed weight loss
327 as a surrogate marker for disease. We found that by 11 days after infection ΔIAP1/2
328 mice lost approximately 20% of their body weight, while all other strains did not (Fig 8A).
329 At this time point and due to ethical constraints, all animals were sacrificed and we
330 analyzed bacterial loads and the immune response in the colon. ΔIAP1/2 mice had
331 significantly higher colonic bacterial load than controls (Fig 8B). This was associated
332 with compromised IL-22 production from the ILC3 compartment (Fig 8C-D).
333 Although ILC3 are important to protect from *C. rodentium* infection, a T_H17 and
334 T_H22 response is also required, as evidenced by susceptibility of $RAG1^{-/-}$ mice to this

335 pathogen (Silberger *et al*, 2017). We therefore additionally analyzed the $CD4^+$ T cell
336 response in the colon. Numbers of total $CD4^+$ T cells were not changed in infected
337 ΔIAP1/2 mice (Fig 8E). However, there was a significant reduction in $ROR\gamma t^+Tbet^-$ $CD4^+$
338 T cells (Fig 8E), which was accompanied by reduced levels of IL-17A (Fig 8F). Despite
339 normal numbers of $ROR\gamma t^+Tbet^+$ $CD4^+$ T cells (Fig 8E), $IL\text{-}17A^+IFN\text{-}\gamma^+$ cells were
340 significantly reduced in infected ΔIAP1/2 mice (Fig 8F). However, production of IL-22
341 was not defective in the absence of cIAP1 and cIAP2 (Fig 8F). Collectively, our data
342 suggest that cIAP1 and cIAP2 are required within the ILC3 and T_H17 compartments to
343 control intestinal bacterial infection.
344

345 **Discussion**

346 In the present study we demonstrate that the E3 ubiquitin ligases cIAP1 and cIAP2 are
347 necessary for γδT17 cells to transition through to prepubescent life by regulating
348 cytokine-mediated proliferation and stable expression of the lineage defining
349 transcription factors cMAF and RORγt. Thus, during aging, cIAP1 and cIAP2 are
350 required in a cell-intrinsic manner to maintain cMAF and RORγt levels and to allow cells
351 to enter cell cycle in response to IL-7, IL-1β and IL-23. Consequently, γδT17-driven
352 inflammatory responses in the skin and draining LNs of prepubescent ΔIAP1/2 mice are
353 blunted despite normal cell numbers, while by the time animals reach adulthood, γδT17
354 populations are deficient in gut, skin and LNs. Mechanistically, our data suggest that
355 this is independent of TNF and TNFR1 and most likely through overt activation of the
356 non-canonical NF-κB pathway. Similar to γδT17, ILC3 required cIAP1 and cIAP2
357 expression during the post-weaning period in order to expand, be maintained until adult
358 life, and induce formation of intestinal ILFs. The ILC3 deficit in ΔIAP1/2 mice together

359 with a defective T_H17 response, correlated with a profound inability to control intestinal
360 bacterial infection.

361 The IL-17-producing γδ T cell subset is an innate-like unconventional lymphocyte
362 that is important in many immunological processes ranging from anti-microbial
363 protection to pathogenic inflammation and cancer (Patil *et al*, 2015). γδT17 cells are
364 pre-programmed and functionally mature in the embryonic thymus in mouse and human
365 (Ribot *et al*, 2009; Haas *et al*, 2012). They are exported into peripheral and secondary
366 lymphoid tissues after birth, and evidence suggests that they go through a second wave
367 of transcriptional and functional programming during neonatal life within the tissues they
368 occupy (Kadekar *et al*, 2020; Wiede *et al*, 2017). The molecular cues that γδT17 cells
369 receive within the tissues during that period are obscure. Our data show that the E3
370 ligases cIAP1 and cIAP2 are required during late neonatal and early prepubescent life
371 in a cell-intrinsic manner for cytokine-induced proliferation, to sustain transcriptional
372 stability and allow optimal inflammatory responses. This work establishes cIAP1/2 as
373 critical molecular regulators of committed tissue-resident γδT17 cells, and underpins the
374 existence and importance of post-thymic temporal events necessary for these cells to
375 be maintained during aging.

376 cIAP1/2 are central for TNFR1 induced canonical NF-κB activation and cell death
377 (Mahoney *et al*, 2008) , and necessary to suppress overt non-canonical NF-κB signaling
378 (Vallabhapurapu *et al*, 2008; Zarnegar *et al*, 2008) . TNFR1 induced apoptosis and
379 necroptosis are fundamental biological processes regulating cell growth during
380 development, homeostatic turnover and even inflammatory diseases (Kalliolias &
381 Ivashkiv, 2016). The two NF-κB pathways on the other hand are synonymous with cell
382 survival, proliferation and differentiation in ubiquitous cell populations (Hayden & Ghosh,

383 2011). In T cells they are mostly active downstream of TNF superfamily receptors and
384 the TCR (Oh & Ghosh, 2013). Although the role of several TNF superfamily receptors
385 and ligands have been studied in γδ T cells (Powolny-Budnicka *et al*, 2011; Shibata *et*
386 *al*, 2011; Silva-Santos *et al*, 2005), the importance of the signaling components of the
387 NF-κB pathway had not been thoroughly investigated. Genetic and pharmacological
388 perturbations of the TNFR1 signaling, combined with aberrant nuclear translocation of
389 RelB that it is the cIAP1/2-mediated control of non-canonical NF-κB that is required for
390 the maintenance of γδT17 cells. This agrees with CD27, a TNF superfamily receptor
391 and potent activator of non-canonical NF-κB (Ramakrishnan *et al*, 2004), suppressing
392 the γδT17 differentiation program (Ribot *et al*, 2009). Importantly, deletion of NIK, the
393 kinase targeted by cIAP1/2 and responsible for activating the non-canonical NF-κB
394 cascade, did not affect γδT17 cell development or homeostasis (Mair *et al*, 2015). This
395 strongly suggests that it is the "brake" imposed by cIAP1/2 in order to avoid over
396 activation of non-canonical NF-κB that is critical and not its baseline activity.
397 There are a number of transcription factors that are important for the development
398 of γδT17 cells (Parker & Ciofani, 2020) . Ciofani and co-workers showed that cMAF acts
399 early in embryogenesis to allow robust expression of RORγt and thus promote
400 specification and stability of the γδT17 lineage (Zuberbuehler *et al*, 2019). How cMAF
401 and RORγt expression is regulated, however, in γδT17 cells is not well-defined. Herein,
402 we demonstrate that loss of cIAP1/2 results in the progressive downmodulation of cMAF
403 and RORγt after birth, providing a molecular understanding of how lineage defining
404 transcription factors are regulated in these cells. Although loss of cMAF and RORγt
405 during embryonic development resulted in rapid loss of γδT17 cells or their progenitors
406 in the thymus (Zuberbuehler *et al*, 2019; Shibata *et al*, 2011) , we observed that in

407 ΔIAP1/2 mice, cells persist for at least 2 weeks without either transcription factor. Thus,
408 it appears that during neonatal life the impact of cMAF and RORγt in γδT17 cells is less
409 pronounced. The exact molecular steps leading to cIAP1/2-dependent regulation of
410 cMAF and RORγt are currently unclear. Our previous work showed that following
411 cIAP1/2 inhibition, NIK-mediated RelB nuclear translocation suppressed expression of
412 cMAF in T_H17 cells (Rizk *et al*, 2019). It is plausible therefore, that accumulation of non-
413 canonical NF-κB signaling directly suppresses cMAF, which subsequently suppresses
414 RORγt. Intriguingly, cytokine stimulation and inflammation could partially restore
415 expression of cMAF and RORγt, indicating a certain degree of transcriptional plasticity.
416 In addition to γδT17 cells, cIAP1/2 were necessary for the establishment of a
417 normal ILC3 population during the post-weaning period in the gut and the formation of
418 ILFs, as well as protection from intestinal extracellular bacterial infection. During
419 infection, we additionally found that cIAP1/2, were critical for the generation of IL-17^+
420 and IL-17^+IFN-γ^+ CD4+ T cells, which have been associated with protection against
421 pathogens, or tissue damage in the context of inflammation (Omenetti *et al*, 2019). We
422 and others have previously reported that the cIAP-non-canonical NF-κB axis is
423 necessary for T_H17 differentiation and successful IL-17-driven responses (Rizk *et al*,
424 2019; Kawalkowska *et al*, 2019), while NIK was shown to be important for the
425 generation of neuropathogenic T_H17 cells (Lacher *et al*, 2018). Moreover, NIK
426 expression and activation of the non-canonical NF-κB pathway in dendritic cells
427 indirectly regulates maintenance of both T_H17 cells and ILC3 (Jie *et al*, 2018). Our
428 current data, extend and broaden the immunological importance of this pathway. We
429 would like to propose that through regulation of non-canonical NF-κB, cIAP1/2 are
430 master regulators of innate and adaptive type-3 immunity. Their requirement is

431 necessary during neonatal life to establish functional innate and innate-like type-3
432 immune cell populations, whereas in the adult they support differentiation of antigen-
433 dependent adaptive type-3 cells.
434
435 **References**

436 Annibaldi A & Meier P (2018) Checkpoints in TNF-Induced Cell Death: Implications in
437 Inflammation and Cancer. *Trends Mol Med* 24: 49–65
438 Annibaldi A, Wicky John S, Vanden Berghe T, Swatek KN, Ruan J, Liccardi G, Bianchi
439 K, Elliott PR, Choi SM, Van Coillie S, *et al* (2018) Ubiquitin-Mediated Regulation of
440 RIPK1 Kinase Activity Independent of IKK and MK2. *Mol Cell* 69: 566-580.e5
441 Bauché D, Joyce-Shaikh B, Fong J, Villarino A V, Ku KS, Jain R, Lee Y-C, Annamalai L,
442 Yearley JH & Cua DJ (2020) IL-23 and IL-2 activation of STAT5 is required for
443 optimal IL-22 production in ILC3s during colitis
444 Bouladoux N, Harrison OJ & Belkaid Y (2017) The Mouse Model of Infection with
445 Citrobacter rodentium. *Curr Protoc Immunol* 119: 19.15.1-19.15.25
446 Cahenzli J, Köller Y, Wyss M, Geuking MB & McCoy KD (2013) Intestinal Microbial
447 Diversity during Early-Life Colonization Shapes Long-Term IgE Levels. *Cell Host*
448 *Microbe* 14: 559–570
449 Cai Y, Shen X, Ding C, Qi C, Li K, Li X, Jala VR, Zhang H ge, Wang T, Zheng J, *et al*
450 (2011) Pivotal Role of Dermal IL-17-Producing gd T Cells in Skin Inflammation.
451 *Immunity* 35: 596–610
452 Cai Y, Xue F, Fleming C, Yang J, Ding C, Ma Y, Liu M, Zhang HG, Zheng J, Xiong N, *et*
453 *al* (2014) Differential developmental requirement and peripheral regulation for
454 dermal Vγ34 and Vγ36T17 cells in health and inflammation. *Nat Commun* 5: 1–14

455 Chen YS, Chen IB, Pham G, Shao TY, Bangar H, Way SS & Haslam DB (2020) IL-17-
456 producing γδ T cells protect against Clostridium difficile infection. *J Clin Invest* 130:
457 2377–2390
458 Conti HR, Peterson AC, Brane L, Huppler AR, Herna´ndez-Santos N, Whibley N, Garg
459 A V., Simpson-Abelson MR, Gibson GA, Mamo AJ, *et al* (2014) Oral-resident
460 natural Th17 cells and γδ T cells control opportunistic Candida albicans infections.
461 *J Exp Med* 211: 2075–2084
462 Eberl G (2016) Immunity by equilibrium. *Nat Rev Immunol* 16: 524–532
463 Eberl G & Litman DR (2004) Thymic origin of intestinal αβ T cells revealed by fate
464 mapping of RORγt+ cells. *Science (80-)* 305: 248–251
465 Fleming C, Cai Y, Sun X, Jala VR, Xue F, Morrissey S, Wei YL, Chien YH, Zhang HG,
466 Haribabu B, *et al* (2017) Microbiota-activated CD103+ DCs stemming from
467 microbiota adaptation specifically drive γδT17 proliferation and activation.
468 *Microbiome* 5: 1–15
469 Gardam S, Turner VM, Anderton H, Limaye S, Basten A, Koentgen F, Vaux DL, Silke J
470 & Brink R (2011) Deletion of cIAP1 and cIAP2 in murine B lymphocytes
471 constitutively activates cell survival pathways and inactivates the germinal center
472 response. *Blood* 117: 4041–4051
473 Guo X, Liang Y, Zhang Y, Lasorella A, Kee BL & Fu YX (2015) Innate Lymphoid Cells
474 Control Early Colonization Resistance against Intestinal Pathogens through ID2-
475 Dependent Regulation of the Microbiota. *Immunity* 42: 731–743
476 Guo X, Qiu J, Tu T, Yang X, Deng L, Anders RA, Zhou L & Fu YX (2014) Induction of
477 innate lymphoid cell-derived interleukin-22 by the transcription factor STAT3
478 mediates protection against intestinal infection. *Immunity*

479 Gury-BenAri M, Thaiss CA, Serafini N, Winter DR, Giladi A, Lara-Astiaso D, Levy M,
480 Salame TM, Weiner A, David E, *et al* (2016) The Spectrum and Regulatory
481 Landscape of Intestinal Innate Lymphoid Cells Are Shaped by the Microbiome. *Cell*
482 166: 1231-1246.e13
483 Haas JD, Malinarich González FH, Schmitz S, Chennupati V, Föhse L, Kremmer E,
484 Förster R & Prinz I (2009) CCR6 and NK1.1 distinguish between IL-17A and IFN-γ-
485 producing γδ effector T cells. *Eur J Immunol* 39: 3488–3497
486 Haas JD, Ravens S, Düber S, Sandrock I, Oberdörfer L, Kashani E, Chennupati V,
487 Föhse L, Naumann R, Weiss S, *et al* (2012) Development of Interleukin-17-
488 Producing γδ T Cells Is Restricted to a Functional Embryonic Wave. *Immunity* 37:
489 48–59
490 Hayden MS & Ghosh S (2011) NF-κB in immunobiology. *Cell Res* 21: 223–244
491 Heilig JS & Tonegawa S (1986) Diversity of murine gamma genes and expression in
492 fetal and adult T lymphocytes. *Nature* 322: 836–840
493 Hoytema van Konijnenburg DP, Reis BS, Pedicord VA, Farache J, Victora GD & Mucida
494 D (2017) Intestinal Epithelial and Intraepithelial T Cell Crosstalk Mediates a
495 Dynamic Response to Infection. *Cell* 171: 783-794.e13
496 Jie Z, Yang JY, Gu M, Wang H, Xie X, Li Y, Liu T, Zhu L, Shi J, Zhang L, *et al* (2018)
497 NIK signaling axis regulates dendritic cell function in intestinal immunity and
498 homeostasis. *Nat Immunol* 19: 1224–1235
499 Kadekar D, Agerholm R, Rizk J, Neubauer HA, Suske T, Maurer B, Viñals MT, Comelli
500 EM, Taibi A, Moriggl R, *et al* (2020) The neonatal microenvironment programs
501 innate γδ T cells through the transcription factor STAT5. *J Clin Invest* 130: 2496–
502 2508

503 Kalliolias GD & Ivashkiv LB (2016) TNF biology, pathogenic mechanisms and emerging
504 therapeutic strategies. *Nat Rev Rheumatol* 12: 49–62
505 Kawalkowska JZ, Ogbechi J, Venables PJ & Williams RO (2019) CIAP1/2 inhibition
506 synergizes with TNF inhibition in autoimmunity by down-regulating IL-17A and
507 inducing Tregs. *Sci Adv* 5: eaaw5422
508 Kiss EA, Vonarbourg C, Kopfmann S, Hobeika E, Finke D, Esser C & Diefenbach A
509 (2011) Natural aryl hydrocarbon receptor ligands control organogenesis of intestinal
510 lymphoid follicles. *Science (80-)* 334: 1561–1565
511 Klose CSN, Kiss EA, Schwierzeck V, Ebert K, Hoyler T, D'Hargues Y, Göppert N,
512 Croxford AL, Waisman A, Tanriver Y, *et al* (2013) A T-bet gradient controls the fate
513 and function of CCR6-RORγt + innate lymphoid cells. *Nature* 494: 261–265
514 Kruglov AA, Grivennikov SI, Kuprash D V., Winsauer C, Prepens S, Seleznik GM, Eberl
515 G, Littman DR, Heikenwalder M, Tumanov A V., *et al* (2013) Nonredundant function
516 of soluble ltα3 produced by innate lymphoid cells in intestinal homeostasis. *Science*
517 *(80-)* 342: 1243–1246
518 Lacher SM, Thurm C, Distler U, Mohebiany AN, Israel N, Kitic M, Ebering A, Tang Y,
519 Klein M, Wabnitz GH, *et al* (2018) NF-κB inducing kinase (NIK) is an essential post-
520 transcriptional regulator of T-cell activation affecting F-actin dynamics and TCR
521 signaling. *J Autoimmun* 94: 110–121
522 St. Leger AJ, Desai J V., Drummond RA, Kugadas A, Almaghrabi F, Silver P,
523 Raychaudhuri K, Gadjeva M, Iwakura Y, Lionakis MS, *et al* (2017) An Ocular
524 Commensal Protects against Corneal Infection by Driving an Interleukin-17
525 Response from Mucosal γδ T Cells. *Immunity* 47: 148-158.e5
526 Mahoney DJ, Cheung HH, Mrad RL, Plenchette S, Simard C, Enwere E, Arora V, Mak

527 TW, Lacasse EC, Waring J, *et al* (2008) Both cIAP1 and cIAP2 regulate TNF -
528 mediated NF- B activation. *Proc Natl Acad Sci* 105: 11778–11783
529 Mair F, Joller S, Hoeppli R, Onder L, Hahn M, Ludewig B, Waisman A & Becher B
530 (2015) The NFκB-inducing kinase is essential for the developmental programming
531 of skin- resident and IL-17-producing Γδ Tδ cells. *Elife* 4
532 Di Marco Barros R, Roberts NA, Dart RJ, Vantourout P, Jandke A, Nussbaumer O,
533 Deban L, Cipolat S, Hart R, Iannitto ML, *et al* (2016) Epithelia Use Butyrophilin-like
534 Molecules to Shape Organ-Specific γδ T Cell Compartments. *Cell* 167: 203-
535 218.e17
536 Matsuzawa A, Tseng PH, Vallabhapurapu S, Luo JL, Zhang W, Wang H, Vignali DAA,
537 Gallagher E & Karin M (2008) Essential cytoplasmic translocation of a cytokine
538 receptor-assembled signaling complex. *Science (80-)* 321: 663–668
539 McGinley AM, Sutton CE, Edwards SC, Leane CM, DeCourcey J, Teijeiro A, Hamilton
540 JA, Boon L, Djouder N & Mills KHG (2020) Interleukin-17A Serves a Priming Role
541 in Autoimmunity by Recruiting IL-1β-Producing Myeloid Cells that Promote
542 Pathogenic T Cells. *Immunity* 52: 342-356.e6
543 Michel M-L, Pang DJ, Haque SFY, Potocnik AJ, Pennington DJ & Hayday AC (2012)
544 Interleukin 7 (IL-7) selectively promotes mouse and human IL-17-producing cells.
545 *Proc Natl Acad Sci* 109: 17549–17554
546 Al Nabhani Z, Dulauroy S, Marques R, Cousu C, Al Bounny S, Déjardin F, Sparwasser
547 T, Bérard M, Cerf-Bensussan N & Eberl G (2019) A Weaning Reaction to
548 Microbiota Is Required for Resistance to Immunopathologies in the Adult Cell Press
549 Oh H & Ghosh S (2013) NF-κB: Roles and regulation in different CD4+ T-cell subsets.
550 *Immunol Rev* 252: 41–51

551 Omenetti S, Bussi C, Metidji A, Iseppon A, Lee S, Tolaini M, Li Y, Kelly G, Chakravarty
552 P, Shoaie S, *et al* (2019) The Intestine Harbors Functionally Distinct Homeostatic
553 Tissue-Resident and Inflammatory Th17 Cells. *Immunity* 51: 77-89.e6
554 Parker ME, Barrera A, Wheaton JD, Zuberbuehler MK, Allan DSJ, Carlyle JR, Reddy
555 TE & Ciofani M (2019) c-Maf regulates the plasticity of group 3 innate lymphoid
556 cells by restraining the type 1 program. *J Exp Med*: jem.20191030
557 Parker ME & Ciofani M (2020) Regulation of γδ T Cell Effector Diversification in the
558 Thymus. *Front Immunol* 11: 42
559 Patil RS, Bhat SA, Dar AA & Chiplunkar S V (2015) The Jekyll and Hyde story of IL17-
560 Producing γδT Cells. *Front Immunol* 6: 37
561 Powolny-Budnicka I, Riemann M, Tänzer S, Schmid RM, Hehlgans T & Weih F (2011)
562 RelA and RelB transcription factors in distinct thymocyte populations control
563 lymphotoxin-dependent interleukin-17 production in γδ T cells. *Immunity* 34: 364–
564 374
565 Ramakrishnan P, Wang W & Wallach D (2004) Receptor-specific signaling for both the
566 alternative and the canonical NF-κB activation pathways by NF-κB-inducing kinase.
567 *Immunity* 21: 477–489
568 Ribot JC, DeBarros A, Pang DJ, Neves JF, Peperzak V, Roberts SJ, Girardi M, Borst J,
569 Hayday AC, Pennington DJ, *et al* (2009) CD27 is a thymic determinant of the
570 balance between interferon-γ- and interleukin 17-producing γδ T cell subsets. *Nat*
571 *Immunol* 10: 427–436
572 Rizk J, Kaplinsky J, Agerholm R, Kadekar D, Ivars F, Agace WW, Wei-Lynn Wong W,
573 Szucs MJ, Myers SA, Carr SA, *et al* (2019) SMAC mimetics promote NIK-
574 dependent inhibition of CD4+ TH17 cell differentiation. *Sci Signal* 12

575 Sandrock I, Reinhardt A, Ravens S, Binz C, Wilharm A, Martins J, Oberdörfer L, Tan L,
576 Lienenklaus S, Zhang B, *et al* (2018) Genetic models reveal origin, persistence and
577 non-redundant functions of IL-17–producing γδ T cells. *J Exp Med* 215: 3006–3018
578 Schindelin J, Arganda-Carreras I, Frise E, Kaynig V, Longair M, Pietzsch T, Preibisch S,
579 Rueden C, Saalfeld S, Schmid B, *et al* (2012) Fiji: an open-source platform for
580 biological-image analysis. *Nat Methods* 9: 676–682
581 Sheridan BS, Romagnoli PA, Pham QM, Fu HH, Alonzo F, Schubert WD, Freitag NE &
582 Lefrançois L (2013) γδ T Cells Exhibit Multifunctional and Protective Memory in
583 Intestinal Tissues. *Immunity* 39: 184–195
584 Shibata K, Yamada H, Sato T, Dejima T, Nakamura M, Ikawa T, Hara H, Yamasaki S,
585 Kageyama R, Iwakura Y, *et al* (2011) Notch-Hes1 pathway is required for the
586 development of IL-17-producing γδ T cells. *Blood* 118: 586–593
587 Silberger DJ, Zindl CL & Weaver CT (2017) Citrobacter rodentium: a model
588 enteropathogen for understanding the interplay of innate and adaptive components
589 of type 3 immunity. *Mucosal Immunol* 10: 1108–1117
590 Silke J & Meier P (2013) Inhibitor of apoptosis(IAP)proteins-modulators of cell death
591 and inflammation. *Cold Spring Harb Perspect Biol* 5: a008730
592 Silva-Santos B, Pennington DJ & Hayday AC (2005) Lymphotoxin-mediated regulation
593 of γδ cell differentiation by αβ T cell progenitors. *Science (80-)* 307: 925–928
594 Spits H, Artis D, Colonna M, Diefenbach A, Di Santo JP, Eberl G, Koyasu S, Locksley
595 RM, McKenzie ANJ, Mebius RE, *et al* (2013) Innate lymphoid cells-a proposal for
596 uniform nomenclature. *Nat Rev Immunol* 13: 145–149
597 Steer CA, Mathä L, Shim H & Takei F (2020) Lung group 2 innate lymphoid cells are
598 trained by endogenous IL-33 in the neonatal period. *JCI Insight* 5

599 Vallabhapurapu S, Matsuzawa A, Zhang W, Tseng P-H, Keats JJ, Wang H, Vignali
600 DAA, Bergsagel PL & Karin M (2008) Nonredundant and complementary functions
601 of TRAF2 and TRAF3 in a ubiquitination cascade that activates NIK-dependent
602 alternative NF-κB signaling. *Nat Immunol* 9: 1364–1370
603 Varfolomeev E, Blankenship JW, Wayson SM, Fedorova A V, Kayagaki N, Garg P,
604 Zobel K, Dynek JN, Elliott LO, Wallweber HJA, *et al* (2007) IAP Antagonists Induce
605 Autoubiquitination of c-IAPs, NF-κB Activation, and TNFα-Dependent Apoptosis.
606 *Cell* 131: 669–681
607 Vince JE, Wong WWL, Khan N, Feltham R, Chau D, Ahmed AU, Benetatos CA,
608 Chunduru SK, Condon SM, McKinlay M, *et al* (2007) IAP Antagonists Target cIAP1
609 to Induce TNFα-Dependent Apoptosis. *Cell* 131: 682–693
610 Wiede F, Dudakov JA, Lu KH, Dodd GT, Butt T, Godfrey DI, Strasser A, Boyd RL &
611 Tiganis T (2017) PTPN2 regulates T cell lineage commitment and αß versus γδ
612 specification. *J Exp Med* 214: 2733–2758
613 Zarnegar BJ, Wang Y, Mahoney DJ, Dempsey PW, Cheung HH, He J, Shiba T, Yang X,
614 Yeh WC, Mak TW, *et al* (2008) Noncanonical NF-κB activation requires coordinated
615 assembly of a regulatory complex of the adaptors cIAP1, cIAP2, TRAF2 and
616 TRAF3 and the kinase NIK. *Nat Immunol* 9: 1371–1378
617 Zuberbuehler MK, Parker ME, Wheaton JD, Espinosa JR, Salzler HR, Park E & Ciofani
618 M (2019) The transcription factor c-Maf is essential for the commitment of IL-17-
619 producing γδ T cells. *Nat Immunol* 20: 73–85
620
621

622 **Materials and methods**

623 **Mice**

624 All animals were bred and maintained in-house at DTU health tech with the approval of
625 the Danish animal experiments inspectorate. cIAP1$^{f/f}$ and cIAP1$^{f/f}$ cIAP2$^{-/-}$ mice were
626 provided by Prof. W. Wei-Lynn Wong at the University of Zurich, Switzerland with the
627 permission of Prof. John Silke, VIC Australia. RORγt^{CRE} mice were provided by Prof.
628 Gerard Eberl at Pasteur Institute, Paris, France. ROSA26-floxSTOPflox-RFP mice were
629 from the Swiss Immunological Mouse Repository (SwImMR). Lymph nodes from
630 TNFR1$^{-/-}$ mice were provided by Prof. William Agace at Lund University, Sweden, while
631 Lymph nodes from cIAP1^{UBA} mutant mice were provided by Prof. Pascal Meier at The
632 Institute of Cancer research, UK.

633 **Cell culture media and buffers**

634 For all preparations of single cell suspensions and cell cultures RPMI 1460 (Invitrogen)
635 supplemented with 10% heat inactivated FBS (GIBCO), 20mM Hepes pH 7.4 (Gibco),
636 50 µM 2-mercaptoethanol, 2 mM L-glutamine (Gibco) and 10,000 U/ mL penicillin-
637 streptomycin (Gibco), was used. Where indicated, IMDM (Invitrogen) was used instead
638 of RPMI 1460 and supplemented as aforementioned. FACS buffer was prepared by
639 supplementing PBS with 3% heat inactivated FBS.

640 **Lymphocyte isolation from mouse organs**

641 Lymphocytes were isolated from peripheral lymph nodes (axial, brachial and inguinal),
642 thymus, ear skin, small intestinal and colonic lamina propria following the previously
643 described protocols (Kadekar *et al*, 2020). Lymphocytes were isolated from cervical and
644 auricular lymph nodes in case of IMQ-induced psoriasis.

645 **Ex-vivo culturing of lymphocytes**

646 For staining of cytokines from lymphocytes that were isolated from peripheral lymph
647 nodes of untreated mice, the cells were plated at a denisty of $10x10^6$ cells /ml in 1ml of
648 supplemented RPMI in 12 well plates. The cells were restimulated with 50ng/ml PMA
649 (phorbol myristate acetate; Sigma Aldrich), 750 ng/ml Ionomycin (Sigma Aldrich) and
650 BD GolgiStop (containing monensin at 1:1000 dilution, BD) and cultured for 3.5 hours at
651 37°C. For estimation of IL-22 production by $CD4^+$ and $\gamma\delta^+$ T cells from homeostatic
652 mice, the lymphocytes were first cultured onvernight with 40ng/ml rmIL-23 (R&D) the
653 restimulated with PMA, Ionomycing and BD GolgiStop as aforementioned. The cells
654 were then harvested and used for flow cytometry staining.
655 In case of lymphocytes that were isolated from peripheral lymph nodes or skin in IMQ-
656 experiments, the cells were plated at a denisty of $5x10^6$ cells /ml in 1ml of supplemented
657 IMDM in 24 well plates. The cells were restimulated with 50ng/ml PMA (phorbol
658 myristate acetate; Sigma Aldrich), 750 ng/ml Ionomycin (Sigma Aldrich) and BD
659 Golgiplug (containing Brefeldin A at 1:1000 dilution, BD) and cultured for 3.5 hours at
660 37°C. The cells were then harvested and used for flow cytometry staining.
661 Alternatively, lymphocytes that were isolated from mesenteric lymph nodes or colonic
662 lamina propria in *Citrobacter rodentium* infection experiments, the cells were plated at a
663 denisty of $5x10^6$ cells /ml in 1ml of supplemented IMDM in 24 well plates. The cells were
664 subsequently treated with 40ng/ml rmIL-23 (R&D) for 3 hours, followed by 50ng/ml PMA
665 (phorbol myristate acetate; Sigma Aldrich), 750 ng/ml Ionomycin (Sigma Aldrich) and
666 BD Golgiplug (containing Brefeldin A at 1:1000 dilution, BD) and cultured for an
667 additional 3.5 hours at 37°C.
668 For cell cycle assay experiments, lymphocytes that were isolated from peripheral lymph
669 nodes of mice, were plated at a denisty of $5x10^6$ cells /ml in 1ml of supplemented RMPI

670 in 24 well plates. The cells were treated with either 20ng/ml rmIL-7 (R&D), or with 10
671 ng/ml rmIL-1β (Biolegend) + 20 ng/ml rmIL-23 (R&D), or 20 ng/ml rhIL-2 (Biolegend), or
672 anti-CD3 (2 µg/ml; clone 145-2C11) for 48 hours. The cells were subsequently
673 harvested for flow cytometry staining.

674 **IMQ-induced psoriasis**

675 Psoriasis was induced in mice by applying 7 mg of Aldara cream (containing 5%
676 imiquimod) to the dorsal side of each ear for 7 days. Histological sections were
677 prepared by fixing ear tissue in 10% formalin overnight and then paraffin embedded.
678 The paraffin embedded sections were cut and stained by H&E.

679 **Flow cytometry staining**

680 Surface antigens, intracellular cytokines and cell cycle assay were stained for flow
681 cytometry as previously described (Rizk *et al*, 2019). For transcription factor staining,
682 the cells were first stained for live/dead discrimination followed by surface antigen
683 staining and subsequently fixed using Foxp3 fixation/permeabilization buffer (Thermo
684 Fisher) for 1 hour at 4°C. The cells were washed once with then stained with the desired
685 antibodies in Foxp3 perm/wash buffer for 1 hour at 4°C. The cells were washed once
686 again and resuspended in FACS buffer and analyzed using BD LSRFortessa.
687 The following antibodies were used herein at 1:200 dilution unless otherwise indicated:
688 Fixed viability stain-700 (FVS700, BD, 1:1000), anti-IL-17A (TC11-18H10; BV786 and
689 PE), anti-IFNγ (XMG1.2; PE-Cy7, APC, BV711 and Percp-cy5.5), anti-IL-22
690 (1H8PWSR; PE), anti-cMAF (symOF1; PE, eF660 or Percp-Cy5.5; 5 µL/test), anti-CD4
691 (GK1.5; BUV395 and FITC), anti-TCRγδ (GL3; BV421 and APC), anti-KLRG1 (2F1 ,
692 BV786), anti-CD27 (LG.3A10; PE-Cy7 and BV650), anti-CCR6 (140706; Alexa Fluor
693 647), anti-CD44 (1M7; V500), anti-CD19 (6D5; FITC), anti-TCRβ (H57-597; APC-

694 eflour780), anti-CD3e (145-2C11, PeCF594 and PE), anti-Tbet(4B10; PeCy7), anti-
695 CD8 (53-6.7;FITC), anti-Vγ5 (536; FITC), anti-Vγ4(UC3-10A6; Percp-eflour710), anti-
696 GATA3(TWAJ; Percp-eFlour710; 1:30), anti-CD45(30-F11;PE and V500), anti-CD127
697 (SB/199; BUV737) and anti-RORγt (B2D; APC and PE).

698 **Administration of Anti-TNF**

699 For neutralization of TNF, 1 week old pups were weighed and i.p. injected with the a-
700 TNF (Adalimumab, brand name HUMIRA) at 5 mg/kg body weight once a week until
701 weaning. After weaning the mice were i.p. injected with 10 mg/kg body weight twice a
702 week until euthanasia at approximately 12 weeks of age.

703 **Transfer of neonatal γδ T cells to RAG1$^{-/-}$ hosts.**

704 First, thymi from 1-2 days old mice were isolated and crushed individually against 70 μm
705 filter to prepare single cell solutions. Subsequently, total γδ T cells were enriched by
706 magnetic depletion of CD4^{+}, CD8^{+}, TCRβ^{+} cells as follows: total thymocytes were re-
707 suspended in MACS buffer at 1e8 cells/ml containing 50 μL/ml normal rat serum and
708 1:200 biotin labelled anti-CD4^{+} (GK1.5), CD8^{+} (53-6.7) and TCRβ^{+} (H57-597)
709 antibodies; the cells were incubated for 10 minutes at room temperature and then
710 incubated with 75 μL/ml EasySep RaphidSphere streptavidin beads (#50001) for 2.5
711 minutes then transferred to EasySep magnet for 2.5 minutes. The non-bound fraction
712 was collected by decantation and centrifugated for 5 minutes at 400g at 4°C.. The
713 enriched γδ T cells from each donor mouse were re-suspended in PBS and then i.v.
714 injected into the tail vein of a RAG1$^{-/-}$ host. The RAG1$^{-/-}$ hosts were euthanized for
715 collection of organs after 12 weeks.

716 **Bone marrow chimeras**

717 The bone marrow cells for reconstitution were isolated by flushing the tibia and femur,
718 which were dissected from donor mice, with culture media. Total bone marrow cells
719 were then centrifuged at 400g for 5 minutes at 4°C. The cells were then re-suspended
720 and passed through 70 μm filter. Subsequently, red blood cells were then lysed using
721 RBC lysis buffer (Biolegend) and a single cell suspension of bone marrow cells was the
722 prepared by passing the cells through 40 μm filter. The prepared cells were then
723 counted and mixed as appropriate.
724 Conversely, host mice were sub-lethally irradiated by 2 doses of 4.5 Gy that were at
725 least 4 hours apart. After 24 hours, the hosts were reconstituted with 10e6 bone marrow
726 cells that were i.v. injected into the tail vein of the host mice. The hosts were euthanized
727 for organs after at least 12 weeks.
728 **Immunofluorescent imaging of intestinal tissue**
729 To assess the presence of SILT in the intestines of WT or ΔIAP1/2 by confocal laser
730 microscopy, the distal ileum was taken and flushed once with HBSS (Thermo Fisher) to
731 remove intestinal contents. Cleaned intestines were fixed for 8h in 4% PFA (Sigma-
732 Aldrich) in PBS and stored in washing buffer (PBS+5%FCS+0.2% Triton X-100 (Sigma-
733 Aldrich)+0.01% Thimerosal (Sigma-Aldrich)) until further use. To prepare the collected
734 intestines for staining, tissues were embedded in 4% UltraPure™ Low Melting Point
735 Agarose (Thermo Fisher) in PBS, sectioned with a swinging blade microtome (Leica
736 VT1200S) into 50 micron sections and permeabilized overnight using the Foxp3
737 Transcription Factor Staining Buffer Set (Thermo Fisher). Permeabilized sections were
738 stained in the supplied permbuffer with an antibody against RORγt (AFKJS-9;
739 unconjugated), followed by a washing step in permbuffer and incubation with a
740 biotinylated secondary antibody against the primary anti- RORγt antibody (Biotinylated

741 anti-rat; Jackson ImmunoResearch). To detect RORγt$^+$ ILC and B cells, sections were
742 washed again in permbuffer and incubated in permbuffer with antibody against B220
743 (RA3-6B2; AF647) and streptavidin-conjugated AF555 (Thermo Fisher), as well as
744 DAPI (Thermo Fisher) to stain all nucleated cells. Sections were washed one more time,
745 mounted on glass slides with ProLong Gold (Thermo Fisher) and analyzed using an
746 LSM710 confocal laser microscope (Carl Zeiss). Images of ≥5 different sections per
747 mouse were acquired with the Zeiss Zen v2.3 software (Carl Zeiss) and analyzed using
748 Imaris v8 (Bitplane/Oxford Instruments) and Fiji v2.1.0/1.53c (Schindelin *et al*, 2012).

749 **Murine *Citrobacter rodentium* infection**

750 Starter cultures of *Citrobacter rodentium* strain DBS100 (ATCC 51459; American Type
751 Culture Collection) were grown overnight at 37°C in Luria-Bertani (LB) medium. The
752 cultures were then used at 5% v/v to inoculate sterile LB medium. The cultures were
753 grown at at 37°C to an OD600 of 0.8- 1 and the CFU count was determined from the
754 OD600 measurement using the following formula: CFU/ml =($5x10^8$)(OD)–$3x10^7$.
755 Subsequently, the bacteria was collected by centrifugation at 4000g for 10 minutes. The
756 bacterial pellet was then resuspended in LB medium to give at $2x10^9$ CFU/100 µL. To
757 infect adult mice, the mice were orally gavaged with either 100 µL of *Citrobacter*
758 *rodentium* or LB control. The mice were weighed before oral gavage and once daily until
759 termination of the experiment. At day 12 post infection all mice were euthanized,
760 dissected to collect organs and fecal samples.
761 The collected fecal samples were weighed and dissolved in PBS and then serially
762 diluted. The serial dilutions were plated on Brilliance™ E. coli/coliform Agar (CM0956,
763 Thermo Fisher) and incubated overnight at 37°C. *Citrobacter rodentium* colonies were
764 identified as being pink colonies and enumerated, while E. coli colonies were identified

765 as purple colonies. CFU/g stool was then calculated as previously described
766 (Bouladoux *et al*, 2017).

767 **Immunofluorescent imaging of nuclear RelB in γδ T cells**

768 Total lymphocytes were isolated from peripheral (axial, brachial and inguinal), cervical
769 and auricular lymph nodes of 4 weeks old mice as described above. Subsequently, total
770 γδ T cells were enriched by magnetic depletion of $CD4^+$, $CD8^+$, $CD19^+$ and $TCR\beta^+$ cells
771 as aforementioned. The cells were then stained with FVS700 for discrimination of live
772 and dead cells and then stained for surface antigens with the following antibodies: anti-
773 TCRγδ (GL3; APC), anti-CD27 (LG.3A10; PE-Cy7) and anti-TCRβ (H57-597; APC-
774 eflour780) all at 1:200 dilution. The cells were subsequently sorted into $TCR\gamma\delta^+$ $CD27^+$
775 or $TCR\gamma\delta^+$ $CD27^-$ cells using BD ARIA-FUSION cell sorter. The sorted cells were
776 collected into cell culture medium and centrifuged at 400g for 5 minutes at 4°C. The
777 cells were then fixed using Foxp3 fixation/permeabilization buffer (Thermo Fisher) for 1
778 hour at 4°C. The cells were washed once with then stained with Foxp3 perm/wash
779 buffer containing anti-TCRγδ (GL3; APC, 1:50), anti-CD3e (145-2C11 or 17A2; biotin,
780 1:100) and anti-RelB (D-4, Santa-cruz, 1:40) for 1-hour 4°C in Foxp3 perm/wash buffer.
781 Again, the cells were washed once and stained with streptavidin-conjugated AF488
782 (Biolegend, 1:100) and anti-mouse AF555 (1:100) for 1 hour 4°C in Foxp3 perm/wash
783 buffer. The cells were then washed once more as previous and stained with DAPI to
784 highlight cell nuclei and washed once more with PBS. Washed cells were mounted on a
785 glass slide using ProLong Gold and imaged with an LSM710 confocal laser microscope
786 and were acquired and analyzed with the Zen v2.3 software and and Fiji v2.1.0/1.53c
787 (Schindelin *et al*, 2012).

788 **Real-Time quantitative PCR**

789 At the indicated timepoints, γδ T cells were sorted from the thymus or lymph nodes of
790 mice directly into RLT buffer mixed with β-mercaptoethanol. RNA was then extracted
791 from using Qiagen RNAeasy microkit following the manufacturer's instructions.
792 Subsequently, cDNA was prepared using BioRad Iscript cDNA synthesis kit using the
793 manufacturer's protocol. Gene expression was then measured by RT-qPCR reactions
794 using BioRad SSOFast EvaGreen supermix, which were run on CFX96 (Biorad) and
795 analyzed using Bio-rad CFX manager software. The following primers were used for
796 RT-qPCR:
797 Actb, Fwd-GGCTGTATTCCCCTCCATCG, Rev- CCAGTTGGTAACAATGCCATGT;
798 RelB, Fwd- GCTGGGAATTGACCCCTACA, Rev- CATGTCGACCTCCTGATGGTT;
799 Birc2, Fwd- TGCCTGTGGTGGGAAACTGA, Rev- GCTCGGGTGAACAGGAACA.
800
801
802

Figures

Figure 1

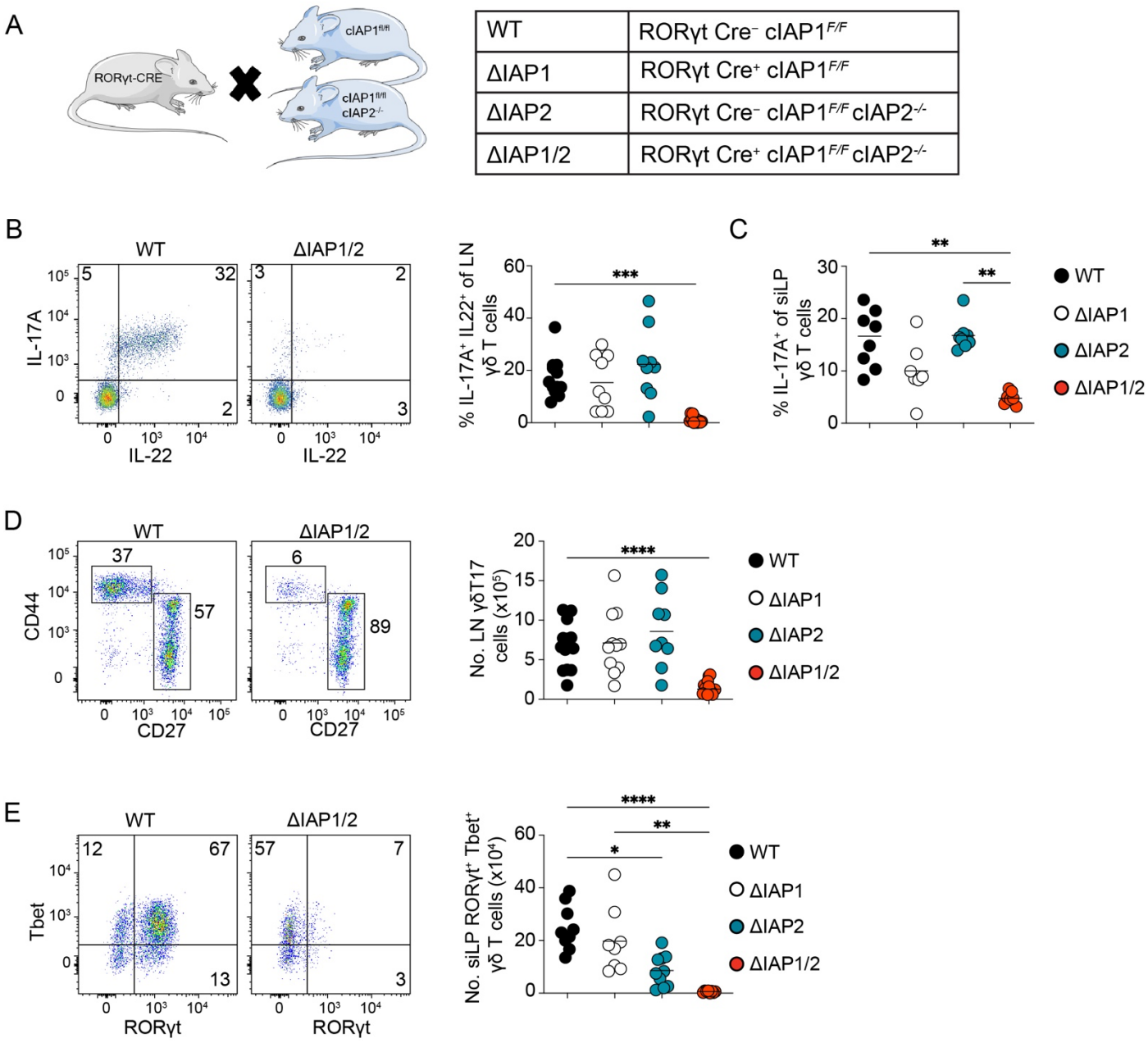

Figure 1. cIAP1 and cIAP2 are required for the homeostasis of γδT17 cells in the LNs and intestinal lamina propria.

(A) Graphical representation of the different mouse strains generated by crossing RORγt^{CRE} mice to cIAP1$^{F/F}$ or cIAP1$^{F/F}$ cIAP2$^{-/-}$ mice. Representative flow cytometric

810 analysis (B) and frequency (B-C) of IL-17^{+} IL-22^{+} cells within γδ T cells in the LNs (B) or
811 (C) IL-17^{+} cells within γδ T in the siLP. (D) Representative flow cytometric analysis (dot
812 plots) and numbers (graph) of γδT17 cells in the LNs of adult WT, ΔIAP1, ΔIAP2 and
813 ΔIAP1/2 mice. (E) Representative flow cytometric analysis (dot plots) and numbers
814 (graph) of RORγt^{+} Tbet^{+} γδ T cells in the siLP of WT, ΔIAP1, ΔIAP2 and ΔIAP1/2 mice.
815 In graphs, each symbol represents a mouse, and lines represent the mean, data is pool
816 of 4 experiments in (B) or 5 experiments in (C-E). *$P < 0.05$, **$P < 0.01$, ***$P < 0.001$,
817 ****$P < 0.0001$ using Kruskal-Wallis test with Dunn's correction.
818
819

820 **Figure 2**

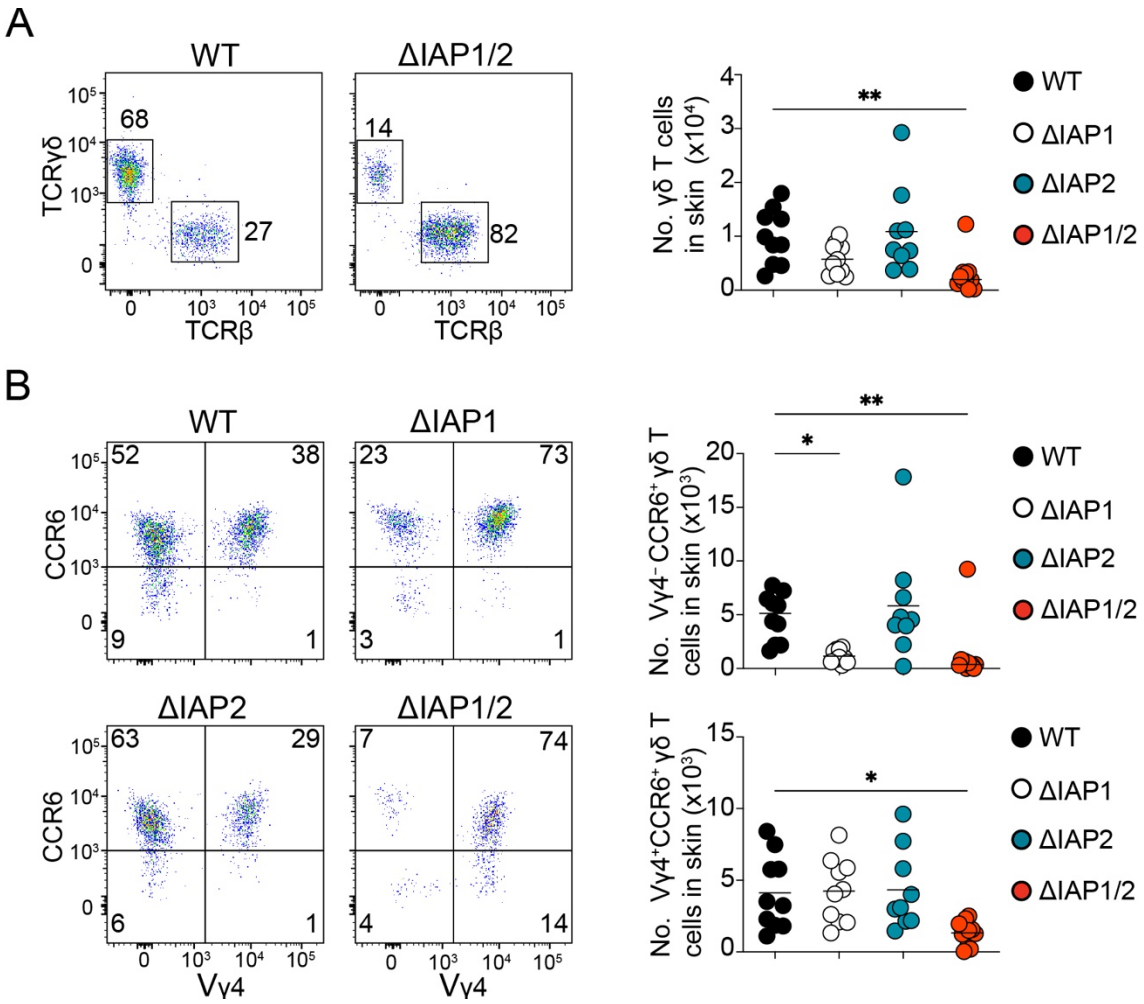

821

822 **Figure 2. cIAP1 and cIAP2 are non-redundantly required for the homeostatic**

823 **maintenance of γδT17 cell subsets in the skin.**

824 Representative flow cytometric analysis (dot plots) and numbers (graphs) of (A) total γδ

825 T cells or (B) $V\gamma4^+$ and $V\gamma4^-$ $CCR6^+$ γδ T cells in the skin of WT, ΔIAP1, ΔIAP2 and

826 ΔIAP1/2 mice. In graphs, each symbol represents a mouse, and lines represent the

827 mean, data is pool of 5 experiments in (A-B). *P < 0.05, **P < 0.01 using Kruskal-Wallis

828 test with Dunn's correction.

829

830 **Figure 3**

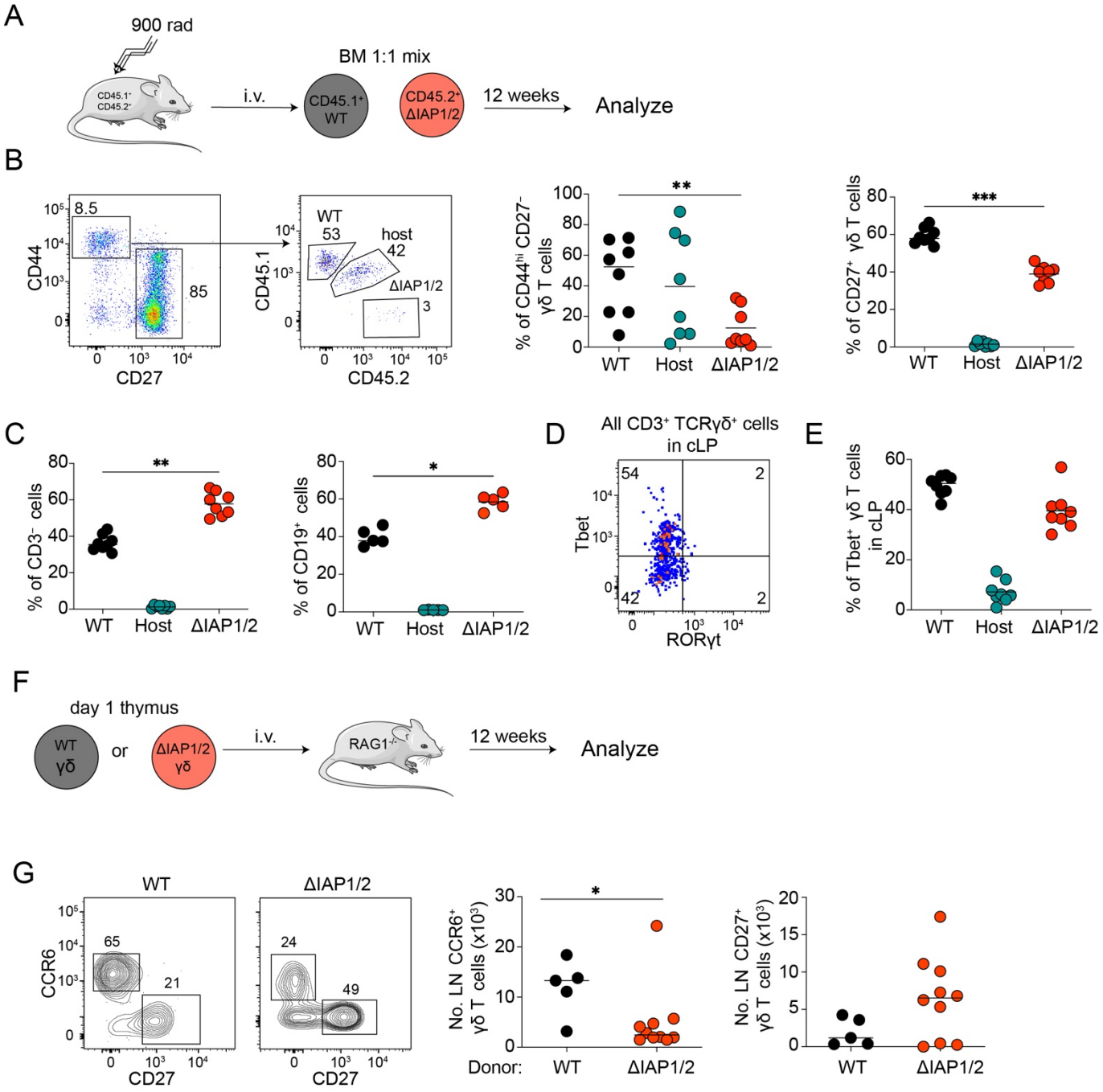

831

832 **Figure 3. cIAP1 and cIAP2 are intrinsically required for the homeostasis of γδT17**

833 **cells.**

834 (A) Graphical representation of the experimental setup for competitive bone marrow

835 experiments. (B) Representative flow cytometric analysis (dot plots) and frequency

836 (graphs) of WT (CD45.1$^+$), host (CD45.1$^+$ CD45.2$^+$) or ΔIAP1/2 (CD45.2$^+$) -derived
837 γδT17 and CD27$^+$ γδ T cells within γδ T cells population in the LNs of reconstituted
838 hosts. (C) Frequency of WT (CD45.1$^+$), host (CD45.1$^+$ CD45.2$^+$) or ΔIAP1/2 (CD45.2$^+$) -
839 derived CD3$^-$ and CD19$^+$ cells in the LNs of reconstituted hosts. (D) Flow cytometric
840 analysis and (E) frequency of RORγt$^+$ and Tbet$^+$ γδ T cells in the cLP of host mice
841 follwing bone marrow reconstitution. (B-E) In graphs, each symbol represents a mouse,
842 and lines represent the mean, data is pool of 3 experiments. *P < 0.05, **P < 0.01, ***P
843 < 0.01 using one-way ANOVA with Tukey's correction. (F) Graphical representation of
844 the experimental setup for transfer of neonatal γδ T cells to RAG1$^{-/-}$ recipients. (G) Flow
845 cytometric analysis (contour plots) and numbers (graphs) of CCR6$^+$ CD27$^-$ or CD27$^+$ γδ
846 T cells in the LNs of RAG1$^{-/-}$ hosts after transfer of neonatal γδ T cells from WT or
847 ΔIAP1/2 pups. In graphs, each symbol represents a mouse, and lines represent the
848 mean, data is pool of 3 experiments (G). *P < 0.05 using Mann-Whitney test.

849

850 **Figure 4**

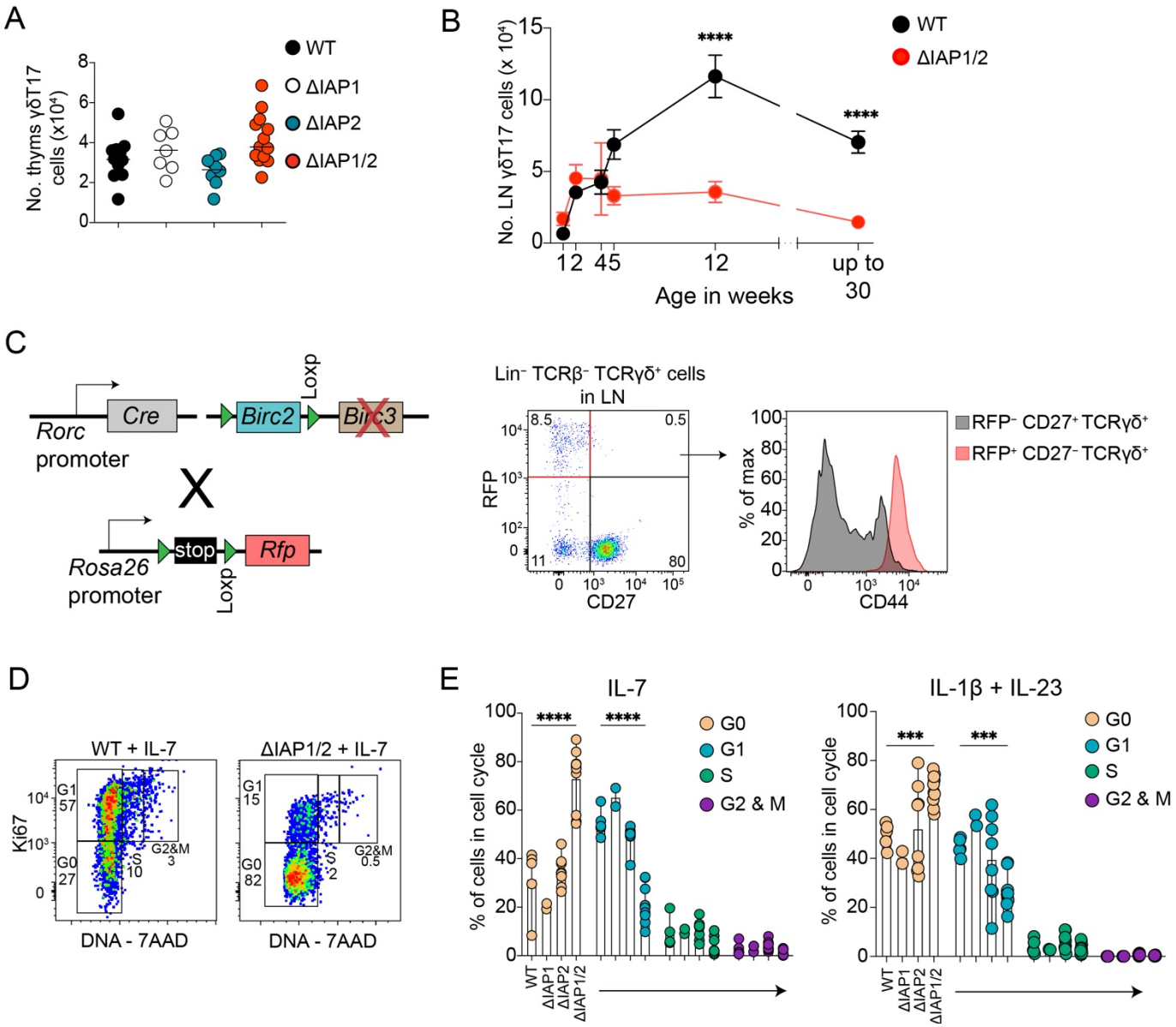

851

852 **Figure 4. cIAP1 and 2 double deficient γδT17 cells are lost progressively during**

853 **aging and fail to progress through cell cycle.**

854 (A) Numbers of γδT17 cells in the thymi of 1-day old WT, ΔIAP1, ΔIAP2 and ΔIAP1/2

855 pups. In graph, each symbol represents a mouse, and lines represent the mean, data is

856 a pool of 3 experiments. (B) Numbers of γδT17 cells in the LN of WT and ΔIAP1/2 at the

857 indicated timepoints. Each symbol represents the mean amalgamated data from each

858 timepoint and the error bars represents the SEM. ****P < 0.01 using Two-way ANOVA

859 with Holm-Sidak correction. (C) Graphical representation of the genetic makeup of the
860 ΔIAP1/2 mice when crossed to the ROSA26-LSL-RFP strain, and representative flow
861 cytometry analysis of LN γδT17 cells from ΔIAP1/2 x ROSA26-LSL-RFP mice. (D)
862 Representative flow cytometric analysis and (E) frequency of cells in G0, G1, S or G2/M
863 cell cycle stages within γδT17 cells that were ex-vivo cultured with the indicated
864 cytokines for 48 hours. In graphs, each symbol represents a mouse, and bars represent
865 the mean, data is pool of 3 experiments. ***$P < 0.001$, ****$P < 0.0001$ using two-way
866 ANOVA with Tukey's correction.
867

868 **Figure 5**

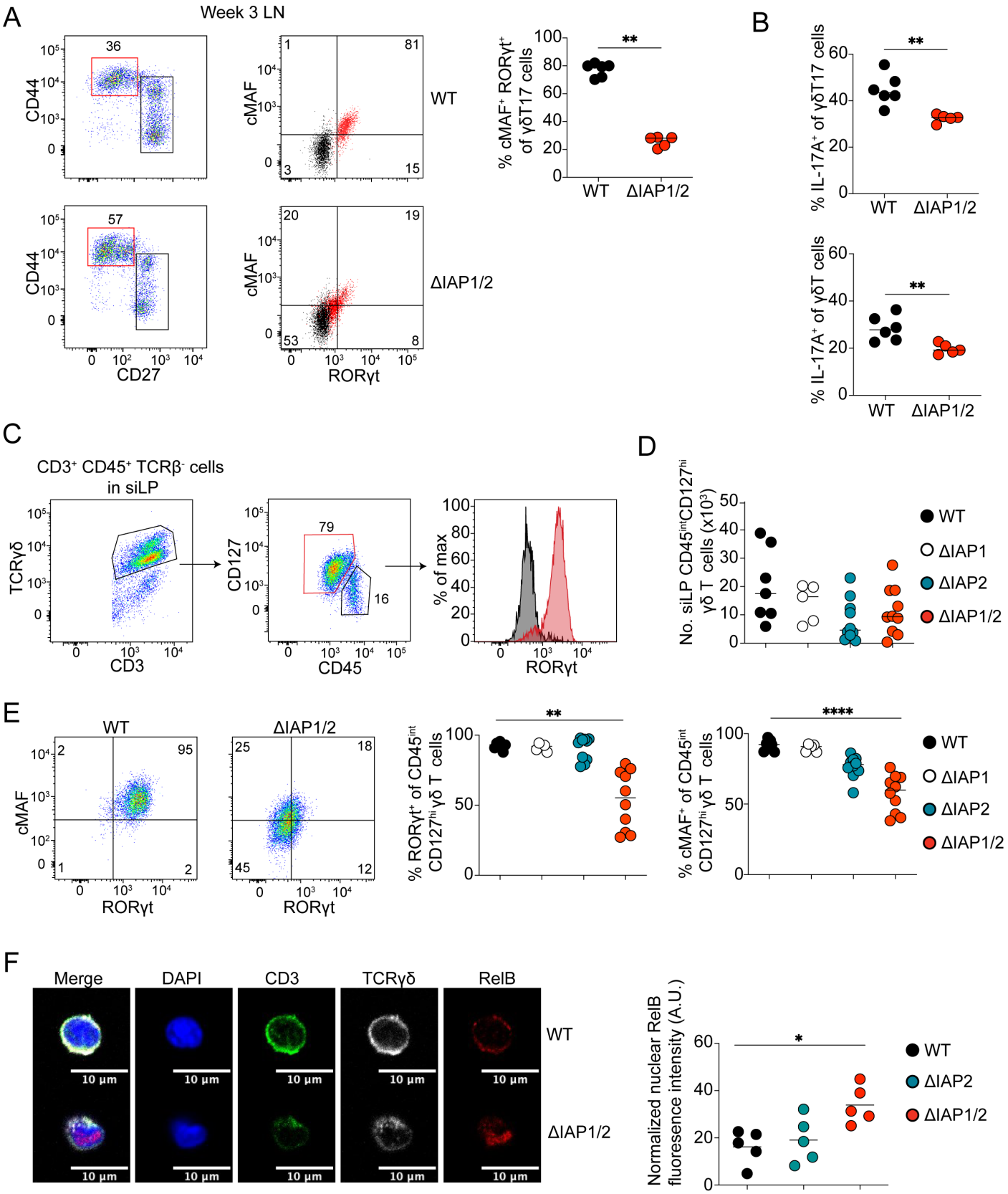

869

870 **Figure 5. cIAP1 and 2 maintain the transcription factor landscape of γδT17 cells in**
871 **the lymph nodes and intestinal lamina propria.**
872 (A) Flow cytometric analysis (dot plots) and frequency (graphs) of RORγt^{+} cMAF^{+} cells
873 within γδT17 cells from the LNs of 3-week-old WT and ΔIAP1/2 mice. (B) frequency of
874 IL-17^{+} cells within γδT17 cells (top) or within all γδ T cells (bottom) from the LNs of 3-
875 week-old WT and ΔIAP1/2 mice. In graphs, each symbol represents a mouse, and the
876 line represent the mean, data is pool of 2 experiments. **P < 0.01 using Mann-Whitney
877 test. (C) Flow cytometric analysis showing the gating strategy and expression of RORγt
878 by CD45^{int} CD127^{+} γδ T cells in siLP of adult WT mice. (D) Numbers of CD45^{int} CD127^{+}
879 γδ T cells in the siLP of 4-week-old WT, ΔIAP1, ΔIAP2 and ΔIAP1/2 mice. (E) Flow
880 cytometric analysis (dot plots) and quantification (graphs) of RORγt or cMAF expression
881 by CD45^{int} CD127^{+} γδ T cells in the siLP of 4-week-old WT, ΔIAP1, ΔIAP2 and ΔIAP1/2
882 mice. In graphs, each symbol represents a mouse, and the line represent the mean,
883 data is pool of 4 experiments. (F) Representative immunofluorescent microscopy
884 analysis of γδT17 cells (CD27^{-} TCRγδ^{+} cells) and normalized nuclear RelB fluorescence
885 intensity in sorted from the LNs of 4-week-old WT or ΔIAP1/2. Images are
886 representative of four independent experiments. *P < 0.05, **P < 0.01, ****P < 0.001
887 using using Kruskal-Wallis test with Dunn's correction.

888 **Figure 6**

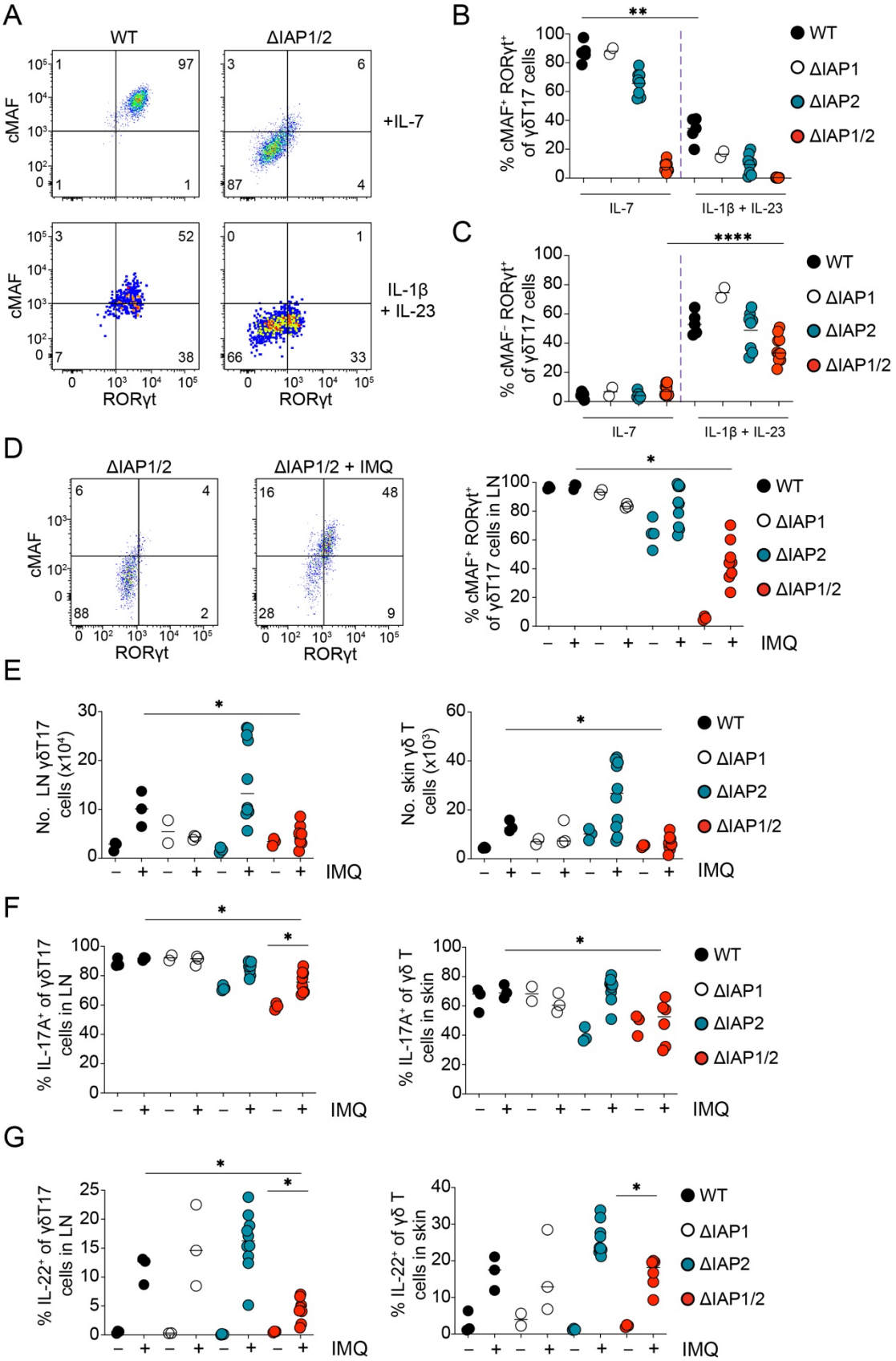

889

890 **Figure 6. Inflammation partially overcomes cIAP1 and cIAP2 deficiency in γδT17**
891 **cells.**
892 (A) Representative flow cytometric analysis and (B-C) quantification of RORγt and
893 cMAF expression by γδT17 cells from the LNs of 4-week-old WT or ΔIAP1/2 mice
894 following ex-vivo culture with the indicated cytokines for 48 hours. In graphs, each
895 symbol represents a mouse, and the line represent the mean, data is pool of 3
896 experiments. (D) Representative flow cytometric analysis (dot plot) and quantification
897 (graph) of RORγt and cMAF expression by γδT17 in LNs of 4-week-old control or IMQ-
898 treated ΔIAP1/2 mice. (E) Numbers of γδT17 cells in the LNs (right) or skin (left) of 4-
899 week-old control or IMQ-treated WT, ΔIAP1, ΔIAP2 or ΔIAP1/2 mice. (F-G) Frequency
900 of IL-17A^{+} (F) or IL-22^{+} (G) cells within γδT17 cells in the LNs or skin of 4-week-old
901 control or IMQ-treated WT, ΔIAP1, ΔIAP2 or ΔIAP1/2 mice. In graphs, each symbol
902 represents a mouse, and the line represent the median, data is pool of 3 experiments.
903 *P< 0.05, **P < 0.01, ****P < 0.0001 using Mann-Whitney test.
904

905 **Figure 7**

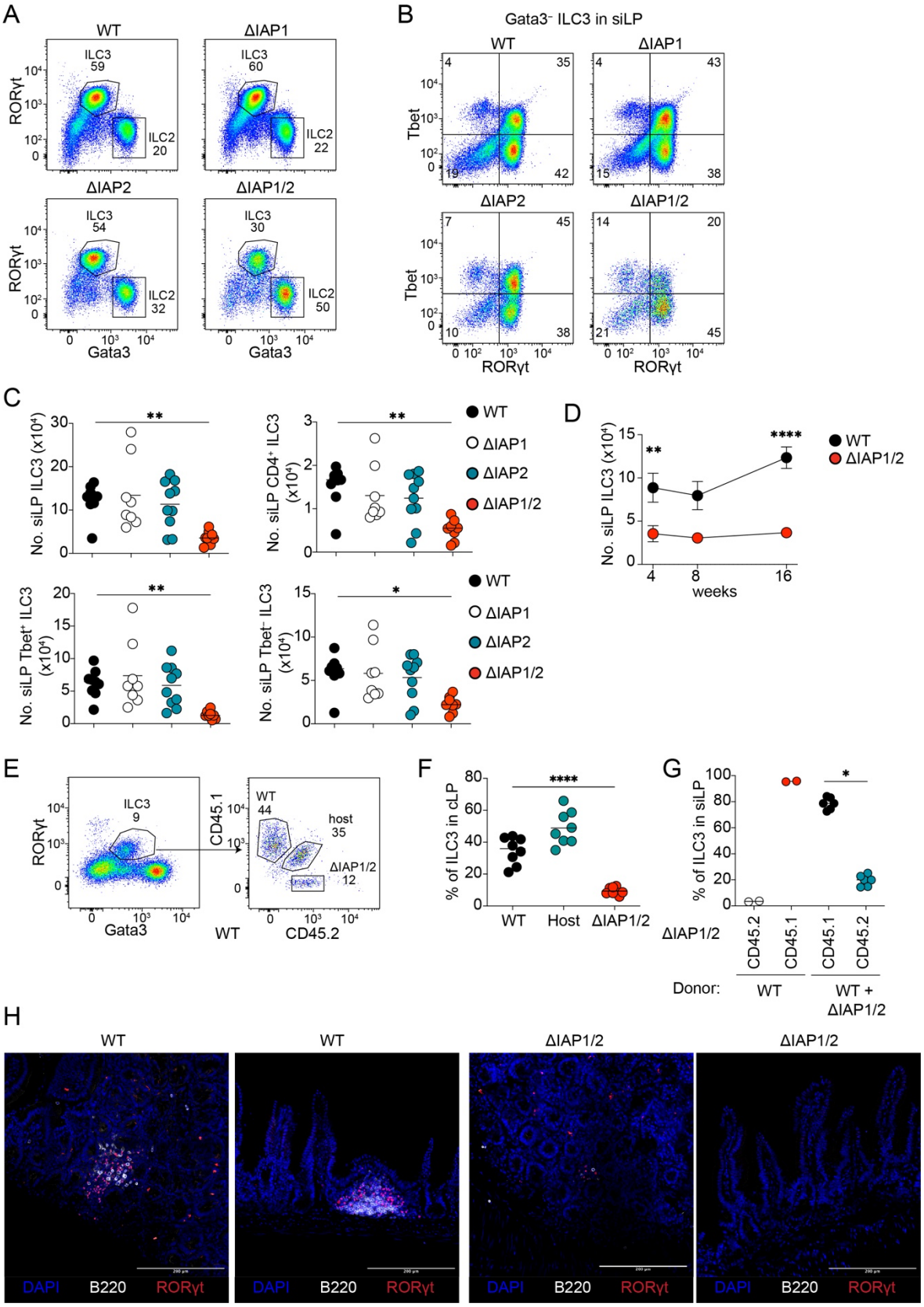

906

907 **Figure 7. cIAP1 and cIAP2 are intrinsically required for the maintanance of**
908 **intestinal ILC3 and for ILF integrity**

909 Representative flow cytometric analysis of (A) total $CD45^+$ $CD3^-$ $CD19^-$ $CD127^+$ ILCs or
910 (B) $CD45^+$ $CD3^-$ $CD19^-$ $CD127^+$ $GATA3^-$ cells in the siLP of adult WT, ΔIAP1, ΔIAP2 or
911 ΔIAP1/2 mice. (C) Numbers of total ILC3s, $CD4^+$, $Tbet^+$ or $Tbet^-$ ILC3s in the siLP of
912 adult WT, ΔIAP1, ΔIAP2 or ΔIAP1/2 mice. In graphs, each symbol represents a mouse,
913 and the line represent the mean, data is pool of 5 experiments. *P< 0.05, **P < 0.01
914 using Kruskal-Wallis test with Dunn's correction. (D) Numbers of ILC3s in the siLP of
915 WT and ΔIAP1/2 at the indicated timepoints. Each symbol represents the mean
916 amalgamated data from each timepoint and the error bars represents the SEM. **P <
917 0.01, ****P < 0.0001 using Two-way ANOVA with Holm-Sidak correction.
918 (E) representative flow cytometric analysis (dot plots) and (F) frequency (graph) of WT
919 ($CD45.1^+$), host ($CD45.1^+$ $CD45.2^+$) or ΔIAP1/2 ($CD45.2^+$)- derived ILC3 in the cLP of
920 reconstituted hosts. In the graph, each symbol represents a mouse, and lines represent
921 the mean, data is pool of 3 experiments. ***P < 0.01 using one-way ANOVA with
922 Tukey's correction. (G) Frequency of WT ($CD45.1^+$) or ΔIAP1/2($CD45.2^+$)- derived ILC3
923 in the siLP of bone marrow reconstituted ΔIAP1/2 hosts. In graph, each symbol
924 represents a mouse, and lines represent the mean, data is pool of 2 experiments. *P <
925 0.05 using Wilcoxon-rank t-test. (H) representative immunofluorescent microscopy
926 images showing ILF structures in distal ileum sections from adult WT or ΔIAP1/2 mice.
927 Images are representative of two independent experiments.

928 **Figure 8**

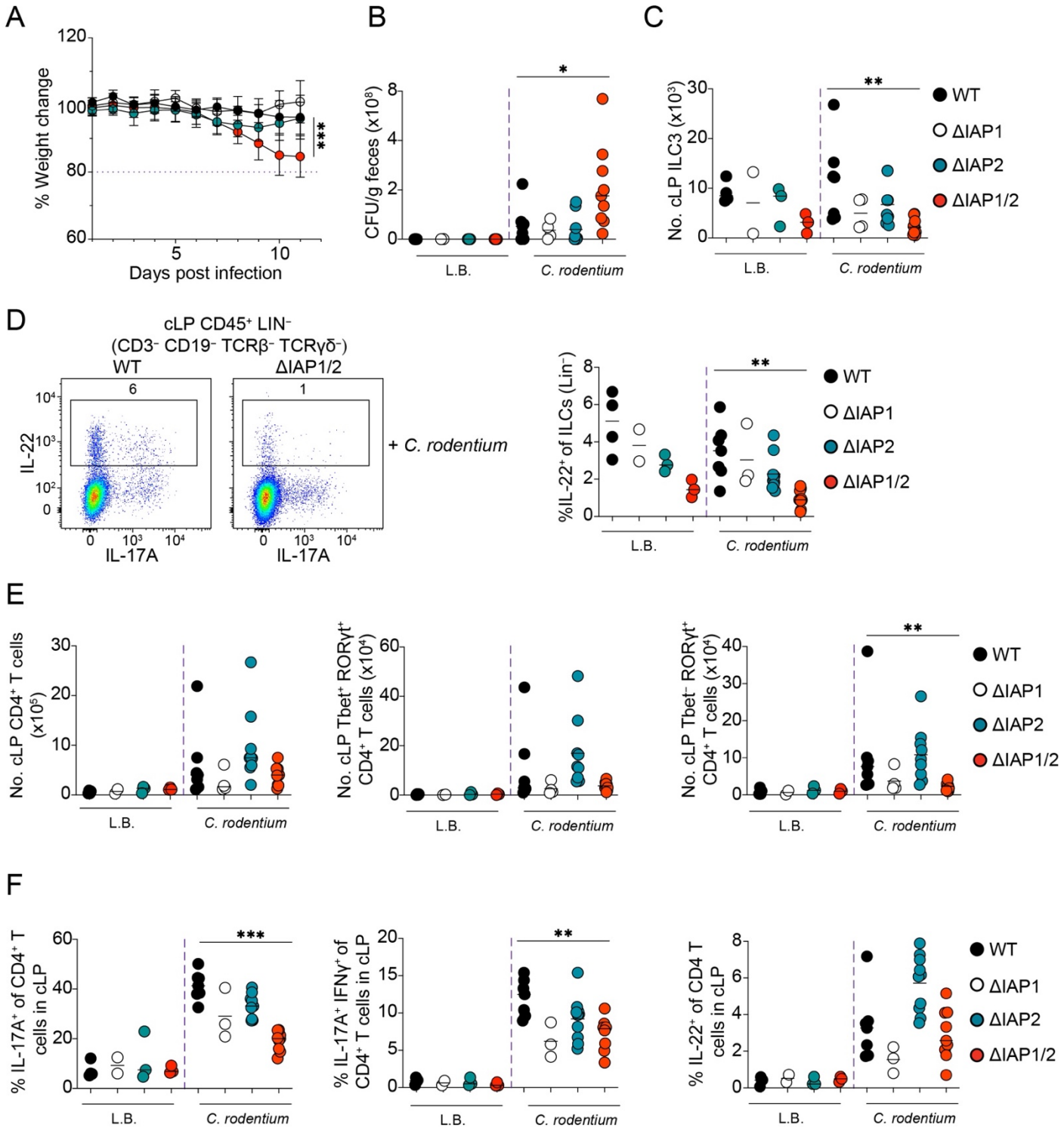

929

930 **Figure 8. RORγt^{Cre+} cIAP1$^{F/F}$ cIAP2$^{-/-}$ succumb to *Citrobacter rodentium* infections.**

931 (A) Percentage body weight change of *C. rodentium* infected WT, ΔIAP1, ΔIAP2 and

932 ΔIAP1/2 mice. Each symbol represents the mean amalgamated data from each

933 timepoint and the error bars represents the SD. ***P < 0.001 using Two-way ANOVA
934 with Holm-Sidak correction. (B) Colony forming units (CFU) of *C. rodentium* in fecal
935 matter of infected and uninfected WT, ΔIAP1, ΔIAP2 and ΔIAP1/2 mice. (C) Numbers of
936 ILC3s in the cLP of infected and uninfected mice. (D) representative flow cytometric
937 analysis (dot blots) and frequency of IL-22$^+$ cells within ILCs in the cLP of *C. rodentium*
938 infected WT and ΔIAP1/2 mice. (E) Numbers of total CD4$^+$ T cells, Tbet$^+$ RORγt$^+$ CD4$^+$
939 T cells, and RORγt$^+$ Tbet- CD4$^+$ T cells in the cLP of infected and uninfected mice. (F)
940 Frequency of IL-17A$^+$, IL-17A$^+$ IFNγ$^+$ or IL-22$^+$ cells within CD4$^+$ T cells in the cLP of
941 infected and uninfected mice. In graphs, each symbol represents a mouse, and lines
942 represent the median, data is pool of 3 experiments. *P < 0.05, **P < 0.01, ***P < 0.001
943 using Mann-Whittney test.